Geologisch-Paläontologisches Institut
und Museum
Christian-Albrechts-Universität
Kiel, Deutschland

Berichte — Reports

Nr. 69

Stüben, Doris; Sedwick, Peter; Savelli, Carlo; Ferretti, Elena;
Wolfson Sensor Group; Geomar Technologie GmbH:

Cruise Report Poseidon 200-4 MIPAMEHR - MAST 1 - Investigations on Hydrothermalism in the Tyrrhenian and Aeolian Sea

Bericht über die Forschungsreise POSEIDON 200-4 MIPAMEHR-MAST
Untersuchungen zum Hydrothermalismus in der Tyrrhenischen See und dem Äolischen Meer

Messina - Messina
29.4. - 12.5.1993

Berichte — Reports, Geol.-Paläont. Inst. Univ. Kiel, Nr. 69,
91 S., 25 Abb., 3 Tab., Kiel, (Juli) 1994

ISSN 0175-9302

Cruise Report Poseidon 200-4 MIPAMEHR - MAST 1 - Investigations on Hydrothermalism in the Tyrrhenian and Aeolian Sea

Bericht über die Forschungsreise POSEIDON 200-4 MIPAMEHR-MAST
Untersuchungen zum Hydrothermalismus in der Tyrrhenischen See und dem Äolischen Meer

Messina - Messina
29.04. - 12.05.1993

Stüben, Doris; Sedwick, Peter; Savelli, Carlo; Ferretti, Elena; Wolfson Sensor Group; Geomar Technologie GmbH

Poseidon 200-4 was a multi-disciplinary expedition (German, English, Italian scientists) with the aim to investigate hydrothermalism in the area of the Tyrrhenian Basin including new exploration technology such as a multisensor ocean floor observation system. This cruise was the final field work within the MAST 1- MIPAMEHR project.

The main objectives of the cruise were:

1. to study and locate the hydrothermal area in the top area of Palinuro and Marsili seamount, to map the hydrothermal plume and to characterize the hydrothermal precipitates.
2. to examine the hydrothermal exhalations around the Aeolian Islands.

It is expected that this study will lead to a better and easier exploration of hydrothermal spots by using a multi-chemical ocean floor observation system as well as to a better understanding of the hydrothermal systems of the Tyrrhenian Sea.

Participants:

Doris Stüben	chief scientist	Geologisch-Paläontologisches Institut, Universität Kiel, Germany,
Peter Sedwick	water chemist	Humboldt fellow
Carlo Savelli	volcanologist	CNR - Instituto di Geologia Marina, Bologna, Italy
Elena Feretti	sedimentologist	Instituto di Geodinamica e Sedimentolgia, Universita degli Studi di Urbino, Italy
Jonathan Barnes	Wolfson Sensor Group	The University of Newcastle upon Tyne Department of Chemistry, Newcastle, England
Jan Norris	"	
Chandra Nauth-Misir	"	
Wolfgang Schneider	technician	Geomar Technologie GmbH, Kiel, Germany
Foster Harps	"	"
Jörg Fließ	"	"
Peter Haushahn	"	ADM Elektronik, Warnau

List of contents

1. Wissenschaftliche Fragestellung

Die Forschungsreise POSEIDON 200-4 ist die dritte Kampagne innerhalb des Projektes "Modular Instrument Package and its Applications in Mediterranean Hydrothermal Research (MIPAMEHR)", das im Rahmen des MAST-1-Programmes von der EG gefördert wird. Wissenschaftliches Ziel war die Auffindung und Evaluierung hydrothermaler Austrittsstellen im Tyrrhenischen Meer (Palinuro, Marsili Seamount) und im Gebiet der Äolischen Inseln.

Forschungsschwerpunkt des MIPAMEHR-Projektes ist die Suche und Erkundung von submarinen Austrittsstellen hydrothermaler Lösungen ("hydrothermal vents" bzw. "hydrothermal plumes") vor allem im Bereich vulkanischer Inselbögen des Mittelmeeres mit Hilfe modularer Instrumentpakete. Der tektonische Rahmen und die Untersuchung von hydrothermalen "Plumes" geben Hinweise auf damit zusammenhängende erzbildende Prozesse am bzw. unter dem Meeresboden. Für die Suche und Lokalisierung von hydrothermalen Austrittsstellen wird neben seismischen, topographischen und magnetischen Indikationen das chemische Signal der hydrothermalen "Plumes" ausgewertet. Dieses soll durch on-line und in-situ Messungen verschiedener Parameter wie z.B. Temperatur, Trübung, gelöstes H_2S, Mn und Fe mittels Sensoren erfolgen. Die Meßergebnisse werden mit Navigationsdaten kombiniert und kartographisch dargestellt, so daß aus der Form und Dimension der Konzentrationsgradienten in Isolinienkarten auf die Lage der hydrothermalen Quellen geschlossen werden kann. Die on-line Meßergebnisse der Sensoren werden durch die Analysen von gleichzeitig genommenen Wasserproben auf weitere "Tracer"-Elemente wie z.B. gelöstes Mn, Fe, Zn und Seltene Erden ergänzt. Nach der Lokalisierung eines submarinen Hydrothermalfeldes erfolgt mit den visuellen Unterwassertechniken des OFOS ("Ocean Floor Observation System") eine detaillierte Untersuchung.

Im Rahmen des MIPAMEHR-Projektes wurde in wissenschaftlich-technischer Zusammenarbeit ein Paket chemischer ASCREV-Sensoren (für Fe, Mn, Zn, Pb) entwickelt (University of Newcastle, England) und in das modifizierte OFOS-Modul (GTG, Kiel) integriert, so daß dieses System später auch von kleineren Forschungsschiffen eingesetzt werden kann. Ein neu implementiertes Transponder-Navigationssystem erlaubt dabei eine sehr genaue Positionierung des OFOS in allen drei Dimensionen.

Die Vorerkundung höffiger submariner Hydrothermalgebiete im Bereich des Tyrrhenischen und Äolischen Meeres war auf der vorangegangenen Expeditionen HYMAS I durchgeführt worden.

Die Forschungsreise POSEIDON 200-4 wurde im Rahmen des MIPAMEHR-Projektes unter zwei Aspekten durchgeführt: erstens sollte ein erstmaliger wissenschaftlicher Einsatz der neuentwickelten Einzelkomponenten - modifiziertes OFOS und Transponder-Navigationssystem, elektrische und ASCREV-Sensoren ("UNT sensor package"), - für sich sowie im Verbund mit

dem gesamten Explorationssystem durchgeführt werden. Zweitens sollte mit diesen neuen Techniken und mit bereits etablierten Methoden das wissenschaftliche Ziel - die Auffindung und Evaluierung hydrothermaler Austrittsstellen im Thyrrenischen und Äolischen Meer - erreicht werden. Insbesondere sollten OFOS-Beobachtungen des Meeresbodens und gleichzeitig direkt übermittelte chemische Sensordaten Aussagen über das Vorkommen von geochemischen Anomalien ermöglichen. Darüberhinaus wurde eine systematische Probennahme durchgeführt, um die hydrothermale Aktivität mit in diesen Gebieten bisher nicht untersuchten geochemischen Parametern detaillierter zu charakterisieren.

2. Cruise schedule POS 200-4

				Scientist
30.4.	19.00	Leaving harbour for Messina Basin		
1.5.	05.00	39°10`N, 15°00` E, WD 2800 m Echosounder profiles S-N, E-W		E. Ferretti C. Savelli
	06.00	Sediment coring 6 m Sediment coring 6 m Sed core 6m Sed core 12 m	POS 335 POS 336 POS 337 POS 338	E. Ferretti C. Savelli F. Harps
	17.00	Transit to Palinuro Seamout 39°28.05`N, 14°48.5`E, 70 m water depth		
	19.00	Profil with 332° Profil with 152° N and back S Profil with 40°,220° Profil with 135°, 315°		
2.5.	05.00	Setting up of the OFOS sensors		I.B. Norris C.R. Nauthm J. Barnes
	09.30	OFOS run at Palinuro seamount for 8 hours at 650 m water depth along the morphology		
	16.00	CTD 700 m water depth		P. Haushahn
	17.00	Deployment of the Transponder		W.Schneider
	20.00	Cruising in the transponder array for calibration		
3.5.	06.00	Sediment grab, 39°32.44, 14°42.3		E. Ferretti
	07.00	Sediment grab, 39° 32.42, 14° 42.4		C. Savelli
	08.00	Sediment grab, 39° 32.50, 14° 42.25		E. Ferretti
	09.00	CTD, 39°32.5, 14°42.25		P. Haushahn
	10.00	Sediment grab, 39°32.0, 14°43.5		C. Savelli
	11.00	Sediment grab, 39°32.0, 14°44.0		E. Ferretti
	12.00	Sediment grab, 39°31.8, 14°44.0		C. Savelli
	12.30	Dredge, 39°31.7, 14°42.3, 950-800 m		F. Harps
	13.00	CTD		P.Haushahn
4.5	03.00	Setting up of the sensors		Newcastle group
	06.00	OFOS, 8h		Schneider
	15.00	MS-CDT		P. Haushahn

	16.00	SL600	F. Harps
	17.00	SL600	F. Harps
5.5	9.00	Lipari	
		Sampling of 750 m site E of Volcano Marsili SMT	
6.5.	6.00	MS, 600 m, 39°16.8, 14°23.95	P. Haushahn
	7.00	DS, 800-500 m on the same spot	F. Harps
	10.00	DS, 39°14.2, 14°22.0, 1100-760m E direction	F. Harps
	13.00	OFOS	Schneider Newcastle group
		Palinuro SMT	
7.5	6.00	OFOS	Schneider Newcastle group
		Transponder collection	
	14.00	SL 600	F. Harps
8.5.		Panarea	
	08.00	Rubber boat to Dattilo-Bottaro 38°38.4, 15°06.3, 30 m	
		CTD, water sampling	P.Haushahn P. Sedwick
		dredging	F. Harps
		Basiluzzo S, CTD, water sampling	
		Basiluzzo, N, 38°40.2, 15°07.6 200 m water depth OFOS	
9.5	08.00	Sampling ashore Salina	P. Sedwick E. Ferretti C. Savelli F. Harps P. Haushahn
	9.00	Profiling W of Lipari	
	11.00	OFOS W Lipari	W.Schneider Newcastle group
	17.30	Picking up people from Salina	
10.5	8.00	W of porto di Ponente on Vulcano	
		CTD with the rubber boat	P. Haushahn D. Stüben

		Water sampling	P. Sedwick
		Poseidon Echosounder profile	C. Savelli
		OFOS test	
	13.00	E of Porto di Levante on Vulcano	
		Water sampling with the rubber boat	
11.5.	09.00	Lipari, harbour master for map return	
	10.00	Transit to Messina	
	14.00	Messina harbour	

Statistics

Total	49	Stations,
including	7	SL sediment-corer-stations,
	8	OFOS Ocean-Floor-Observation-System-stations,
	7	MS multiprobe + water rosette- stations,
	2	Transponder stations,
	12	BG sediment-grab-stations,
	4	DS dredge-stations
	2	Stations from the rubber boat,
	4	WS niskin-water-sampler-stations,
	3	Profil-/echosounder-stations

3. Geological Setting of the Tyrrhenian Sea

The Tyrrhenian Basin, enclosed by the Italian peninsula to the northeast, Sicily to the south, and the Sardinia-Corsica high to the west is a topographic low with depths in excess of 3500 m (Fig. 1). The center of the basin is characterized by bathyal plains (Vavilov and Marsili plains) resulting from Plio-Quarternary turbidite deposition, and large mounts and ridges rising above the bathyal plain. These highs, parallel to major fault trends, represent tilted continental blocks and volcanic highs.

The Tyrrhenian Basin has developed as a marginal basin through drifting of the Calabrian-Sicilian arc system towards the east-southeast. The main structural features of the basin result from this movement. The tensional structures (normal faults) of the margins are mainly aligned N10° to N30°E; the transform faults are oriented N110°-N120°E. Except for a previous structuralization linked to the Western Mediterranean rifting and drifting, the first extensional movements affected the Tyrrhenian area as early as Lower Miocene time, during the post-Burdigalian. Nevertheless, the main rifting phase, which led to oceanic accretion was initiated during the Late Tortonian. The narrow central oceanic area, generated mainly around the Early Pliocene, is restricted to the rift's axis.

The marginal basin type of evolution of the Tyrrhenian Sea is most probably directly linked to subduction of the Ionian lithosphere. Nevertheless, interferences between collision in the surrounding Apennines, Calabria of Sicilides and subduction processes have dominated this special back-arc basin evolution. Since Late Tortonian time, the Tyrrhenian arc shows a regional N120°E-oriented tensional pattern. Short compressional events occur briefly in Middle Pliocene and Middle Pleistocene times, correlated with brief paroxysmal phases of extension and subsidence. The deformation depends on the presence of a subduction zone parallel to the Calabrian arc swell which allows the migration of the unblocked segments of the arc in a N120°E direction (Rehault et al., 1987).

In the Southeastern Tyrrhenian Sea is located a sequence of volcanic islands and seamounts which form the concave arc of the Aeolie (Fig. 1). The Marsili deep basin borders the internal side of this arc. Both the interarc basin and the island arc developed within the Alpine/ Apennine collisional orogens related to a WNW dipping Benioff zone. The seismogenic zone and the supra-subduction magmatic manifestations have migrated away from the volcanic arc of the Sardo-Corso continental block in accordance with the diachronous opening of the southern Tyrrhenian deep basins of Vavilov and Marsili.

A tectonic regime characterized by collapse and crustal extension was associated with the development of magmatic activity in the Southern Tyrrhenian volcanic area. The magnetic zone in the deep plains is, on the whole, characterized (Agip 1981; Arisi Rota and Fichera, 1987) by an

average wavelength of the anomalies of 30 km and amplituede of 200 nT and more. The zone has a basic substratum of high susceptibility (from 150 to 350 SI unit x 10^{-5}). On the whole, this basement is well distinguishable from the continental magnetic zone of the Tyrrhenian margins notwithstanding the presence of some areas possessing a gradual variation of the magnetization.

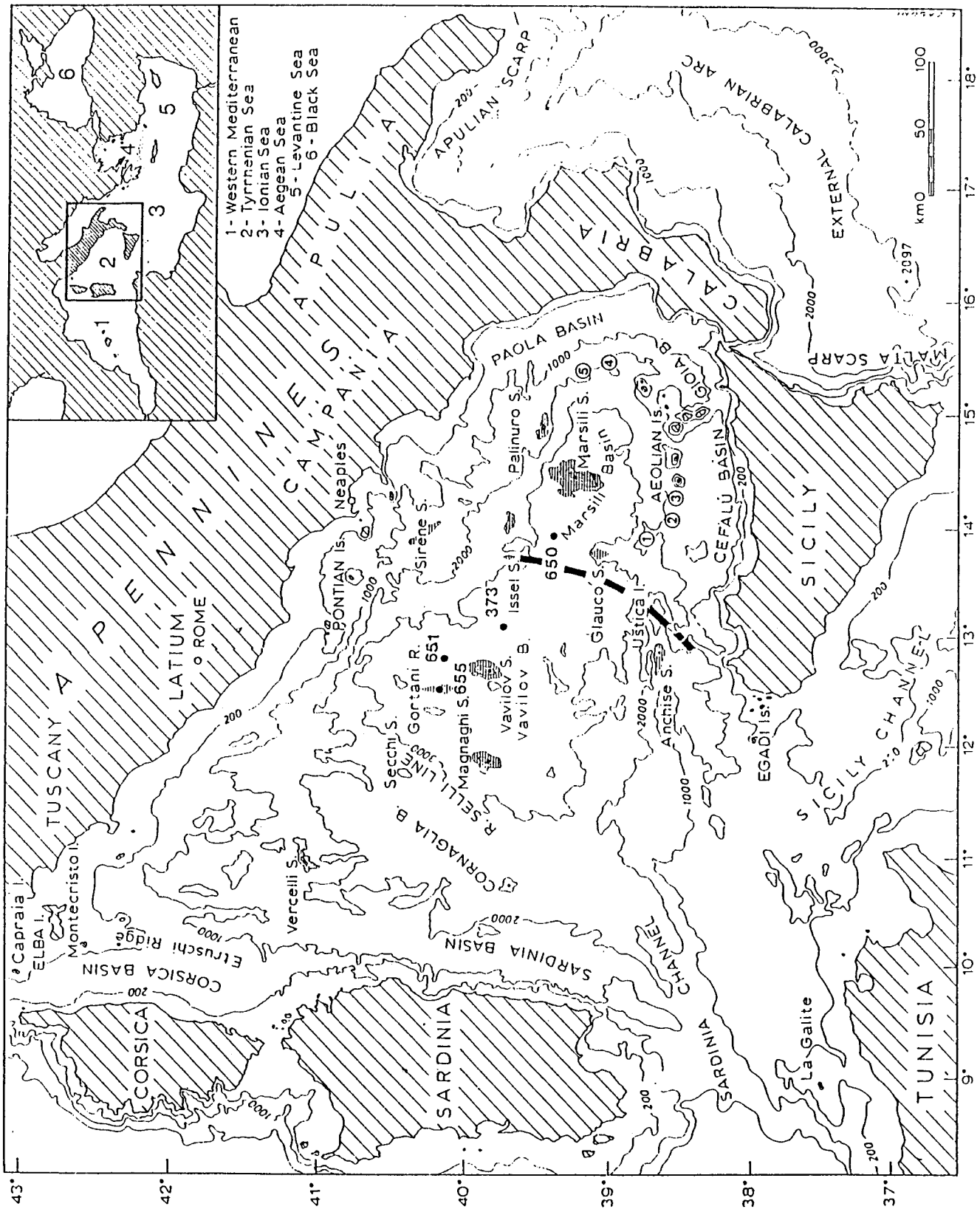

Fig 1 Tyrrhenian Sea

Strike-slip magmato-tectonic lineations

Overall, the Tyrrhenian Sea is crossed by important, deep fault systems and affected by spreading mechanisms which are probably still acting. Two great east-west trending strike-slip tones are located to the north and south of the Marsili deep basin (Boccaletti et al., 1984, 1990; Finetti and Del Ben, 1986; Lavecchia 1988; Savelli and Schreider, 1991; Locardi and Nicolich, 1992). They are known, respectively, as the Palinuro and as the north Sicilian slope lineation zones.

The diachronous emplacements of oceanic crust flooring the Vavilov and Marsili deep basins suggest a migration of the Tyrrhenian seafloor magmatism from west to east. The inferred existence of a central Tyrrhenian arc sited along the structural discontinuity, i.e., between the two bathyal plains may be due to a jump of the active spreading zone (Rehault et al., 1987; Kastens et al., 1988). In particular this process can be characterized by propagation of the opening across east-west sinistral strike-slip faults converging into one tone /scattered strike-slip faults). The Tyrrhenian opening appears to be complicated by the existence of a large strike-slip component to the spreading processes. The seep-seated east-west trending strike-slip faults separate the southern areas of the Tyrrhenian seafloor, which were affected by greater intensities of the opening, and extension movements from the adjoining northern areas. It can be observed from the magnetic pattern that one such strike-slip zone straddles the marginal areas situated respectively to the south and north of the volcanoes Vavilov and Marsili,and continues to the east to Palinuro seamount (Colantoni et al., 1981). This seamount could represent a volcano created on a deep leaky strike-slip zone (Boccaletti et al., 1984; Finetti and Del Ben, 1986; Lavecchia 1988). Another first order E-W strike-slip alignment zone borders the Deep of Marsili to the south. Along this zone, to the west of the NW-SE trending silands of Salina-Lipari-Vulcano, were emplaced the old reliefs of the Aeolian volcanic arc. The left-lateral motions of the magmato-tectonic lineation zones are associated with the development of clockwise rotations (Doglioni 1991) of the adjacent fault-blocks which were originally N-S trending and acquired late NE-SW orientations.

3.1. Palinuro volcano

Perityrrhenian volcanic complexes, among which a certain number are marine, are aligned from Tuscany to Campania along the internal side of the Apenninic chain. To the south of this alignment, the well known Aeolian island-arc, with its typical calcalkaline orogenic volcanism (Beccaluva et al., 1985), is bounded to the west by the Ustica island and Anchise seamount. All these volcanic complexes are encompassed by the compressional front of the Appenines Maghrebian nappes. The Aeolian volcanism, of which the Palinuro volcano could represent the northermost counterpart, consists of seven islands and several seamounts lying on the Sicilian-Calabrian continental slope which grades northwestward to the Southern Tyrrhenian abyssal plain (Marsili Basin). This volcanism structurally belongs to the Calabrian arc which reached its present

configuration in Upper Pliocene and represents the connection between the NW-ES trending Apennines and E-W trending Maghrebides (Beccaluva et al., 1985). The Palinuro seamount (Colantoni et al., 1981), consisting of an array of volcanic edifices (Fig. 2), is emplaced along the E-W trending fault system extending seaward of the northern limit of the Calabrian arc. To the north the relief bounds the continental slope of the southern Apennines and to the south directly faces the Tyrrhenian bathyal plain, sharply separating two different first order physiographic and structural elements and indicating that the generating fracture system could be deeply seated. The seamount has an elongated, roughly elliptical shape, with its major axis extending some 50 km in an E-W direction. It raises about 2000 m above seafloor north of the ridge and more than 3200 m above seafloor SW of it. Individual peaks rise to fairly shallow depths below sea surface (Fig. 2). The complex can be divided into two zones: a) one corresponding to the eastern part of the edifice, with its summit situated at about 70m; and the other culminating at a depth of about 600m, making up the central western part of the seamount and extending E-W (this lineation coincides with the main fault systems) for a distance of about 20 km (Minniti and Bonavia, 1984). Secondary fractures and dislocations are present, extending N-S and NNE-SSW (Colantoni et al., 1981).

The morphologies reveal perfectly circular or broken forms (calderas?). The centres of eruption present are clearly identifiable as summits, in comparison to the tormented shapes of the areas around them. The sides of the craters are scarred by structures radiating from the crater mouths; on the crests, what are probably structural lineations separated by thalwegs that are more or less filled with sediments can be seen. In fact, the surface of seafloor is covered by a yellowish-gray to brown-olive sediment. The thickness of sediments ranges from 0-2m at 400m water depth to 1-3m at 600m water depth. Local irregular patches of white or light yellow colour on the sediments surface are indicative of past and/or present hydrothermal activity. The thickness of these sediments, often containing abundant Fe-oxydes, seems to be greater on the western, deeper part of the seamount.

In more detail, the morphobathymetric features of the Palinuro volcano (Fig. 2) suggest a splitting of the relief, at about 14°45' east, into two parallel elongate structures, about 4 nautical miles in a N-S direction from each other. The southern (and eastern) physiographic elongation is shallow and related to the positive magnetic anomaly of high intensity (up to about 300 nT; AGIP 1981). The northern deeper one culminates at about 570m and contains the weaker positive anomaly (100 nT).

The Palinuro seamount has been the subject of several studies in the past, starting in the seventies. Until 1984, most of the studies on this area were aimed to the geomorphologic and petrologic characteristics of the mount (Selli 1970; Ciabatti, 1970; Del Monte 1972; Fabbri et al., 1973; Di Girolamo 1978), as well as to the newly discovered iron and manganese-crusts

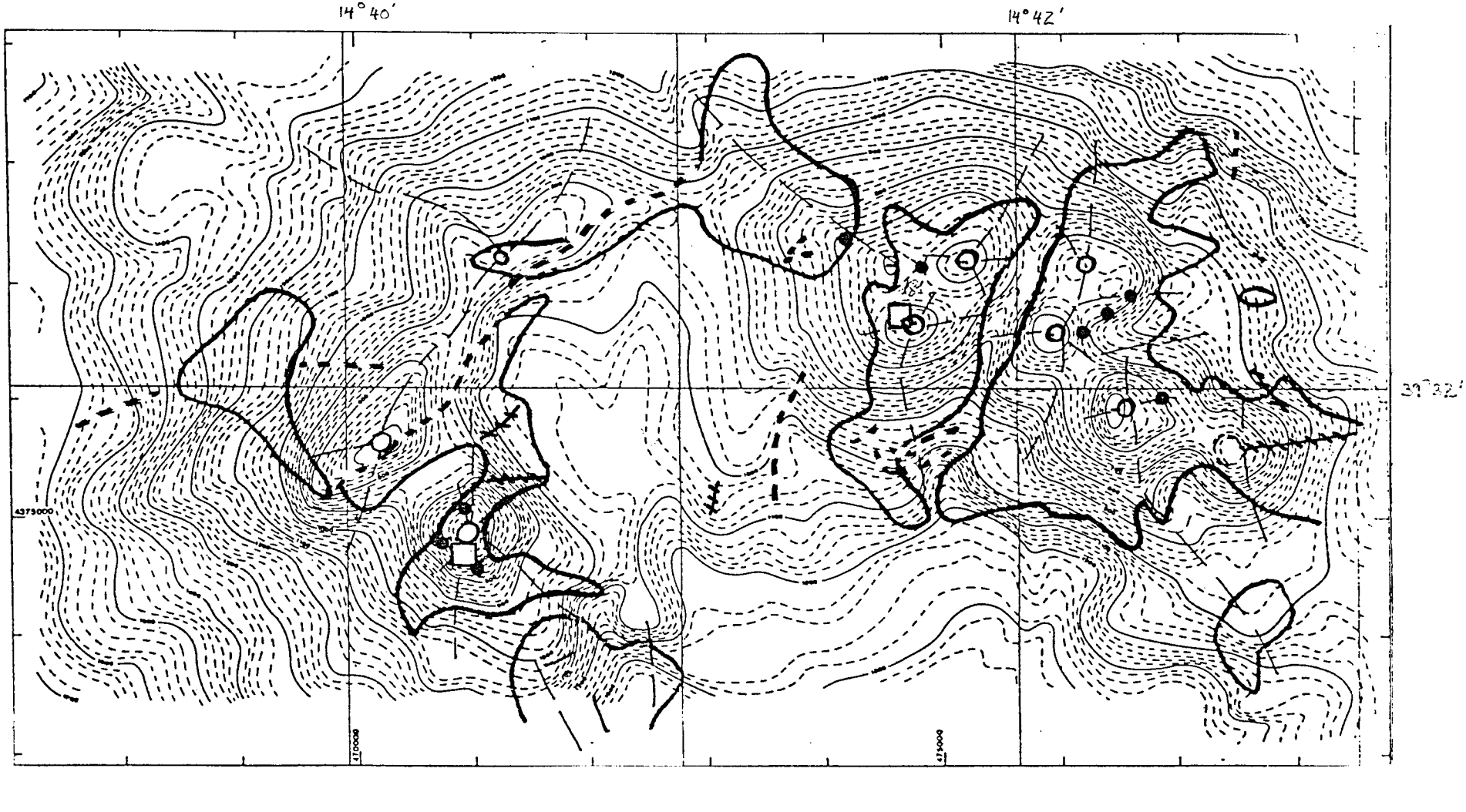

Fig 2 **M. Palinuro - Zona A - Scala 1:50.000**

- crateri
- colate
- fratture raggiate
- faglie (?)
- fronti di colata (?)
- solfuri

occurring both on the Palinuro and other seamounts nearby (Rabbi 1970; Kidd and Armansson, 1979; Selli and Gabbianelli, 1979; Bocchi et al., 1979; Rossi et al., 1980; Morten et al., 1980). After the experience of the Mn-findings, at the beginning of the eigthies, the Italian State-owned company Samim Ocean Inc., decided to initiate a study on the economic potential of manganese deposits within the territorial waters. The preliminary exploration campaignes pursued the ultimate aim of identifying the limits of promising areas where crusts and nodules were to be found. During these prospections were firstly identified the crater-like structures, followed by the discovery of widespread copper anomalies in the sediments outside crater structures, and eventually by the accidental recovery by gravity sampling (Nereide method) of blocks of massive sulfides (Minniti and Bonavia, 1984) on the western edge of the seamount (Fig. 2), at water depths between 600 and 400m. During the sampling campaign by Asmim Ocean both the Kullenberg and Nereide gravity corers had been used, the first one capable of performing core operations in soft sediments to 3-4 meters in depth, the second one for sampling in less deep, but heavily indurated lithologies. Echo-sounders (TEF and Sparker) and the long range side-scan soner (SOL 120) were employed to gain information about sediment stratigraphy and to reconstruct the morphology of the volcanic complex. Some parts of the explored area were observed visually by manned and unmanned submersible craft and all traverses were recorded by camera.

Few years later, the German vessel SONNE returned to the Palinuro samount (Cruise SO41) (HYMAS I, 1986), under the leadership of the Institut für Petrographie und Geochemie of the Univerity of Karlsruhe (Prof. H. Puchelt). Owing to shortage in time and the limits on activity permitted, the SONNE cruise focused on the more central part of Palinuro (Fig. 2), where a carefully navigated seafloor survey was carried out. The instrument used was a photosledge (OFOS) by PREUSSAG-Meerestechnik; using this tool the topography and surface of the seamount could not only be observed, but also recorded in videotape or by colour photographs along the respective track. Some interesting places found during OFOS tracks were then sampled with the television grab, also developed by PREUSSAG. Moreover, within the accessible areas of Palinuro, several detail mapping by SEABEAM technique were performed. Recovered were, beside brown patches and crusts of manganese-iron oxydes, large pieces (up to 25kg) of massive sulfides, generally embedded in olive-grey sediment, at a water depth of about 600m. The recovery of sulfide pieces occurred again in the western side of the seamount (Fig. 2), even in a more easterly position within the structure, compared with the recovery point of Minniti and Bonavia (1984). The last two authors did not mention any striking evidence of ongoing hydrothermal activity in the whole area (like black smokers or powerful fumaroles). An intense precipitation of flocculant material, white or yellow in colour, resulting in silica and barite precipitates, as well as the occurrences of higher density brines, were observed close to the mineralized area. The presence of different colouring in the sedimentary-volcanic ooze containing the sulfides, accompanied by well terminated quartz crystals and Fe-smectite, and especially the occurrence of the sulfides themselves, is a clear evidence of a fairly recent hydrothermal activity,

possibly focused along well defined directions. A thermal measurement, performed in the brine pool indicated water temperature of 182°C. In the Report of the SONNE 1986 Cruise (HYMAS I, 1986), a few indications of hydrothermal activity are given again. Heat flow measurements in this area, although performed, were not successful. The only evidences of hydrothermal processes consist of yellow and white precipitates, accompanied by Mn-crusts.

Hard rock recovery from Palinuro Volcano has been demonstrated to be a rarely successful operation owing to sediment abundance, a common characteristic of Tyrrhenian seamounts. The fact that available lava samples are limited to the top portion any conclusion makes it difficult to extrapolate to the whole volcanic structure. Lavas of Palinuro seamount were sampled only in three sites. From the geochemical point of view, the recovered rocks consist of basaltic andesites and andesites of calcalkaline, subduction-related composition. On a fresh sample of silica-poor andesite dredged from the mount an age of 0.35 +/- 0.05 Ma was determined (Colantoni et al., 1981).

The initial stages of formation of the oceanic basements in the two deep basins of Tyrrhenian sea were likely characterized by a stress field of strong extension within an oceanic rift valley environment at about 70km wide and at a waterdepth considerably shallower than the present one. The associated diffuse-type low-intensity anomalies are akin to those which form the so called uncorrelatable "magnetic quiet zone" observed in young areas of rifting, flanking the spreading axis (Cochran 1981). They may have been displaced by linear high-intensity anomalies accompanying the volcanic manifestations of the axial oceanic accretion. In the bathyal plains of Tyrrhenian sea a process of spreading, comparable with that described above, seems to have taken place. In fact, the great ridges of Marsili and Vavilov, associated with elongate, high-intensity anomalies, have been emplaced in approximately central locations relative to the former spreading of the low-lying basaltic crust characterized by round-shaped magnetic configurations. The overall spreading velocity of the bathyal plains can be estimated to be about 4.4 cm/a in the east-west direction of maximum extension.

As documented by the previous drillings, the igneous crusts flooring the two Tyrrhenian backarc deep basins, around the volcanoes of Vavilov and Marsili, show diversity of composition. It has been indicated (Bertrand et al., 1990; Beccaluva et al., 1990) that this chemical complexity reflects primarily the different nature of magma sources existing in the two basins indicative by the MORB producing mantle diapir of the Vavilov (ODP Sites 373 and 655) and the supra-subduction metasomatized mantle wedge affecting both the Marsili (Site 640) and the northern part of Vavilow (Site 651).

Chronological data now available (Savelli 1988; Feraud 1990) clearly indicate a diachronous activity, that is the interarc volcanism of both the Vavilov and Marsili abyssal plains developed after the magmatic activity ceased in the adjacent remnant arc on the west and before it started in

the new one on the east. Also in the Mariana arc-backarc sequences, during the early stages of interarc basin opening, arc-related volcanism is absent both on the remnant arc and the migrating forearc plate. Despite the significant differences concering the crustal basement and the respective geological frameworks, the Tyrrhenian basin and the above-mentioned region shares fundamental analogies, in terms of timing of tectono-magmatic events.

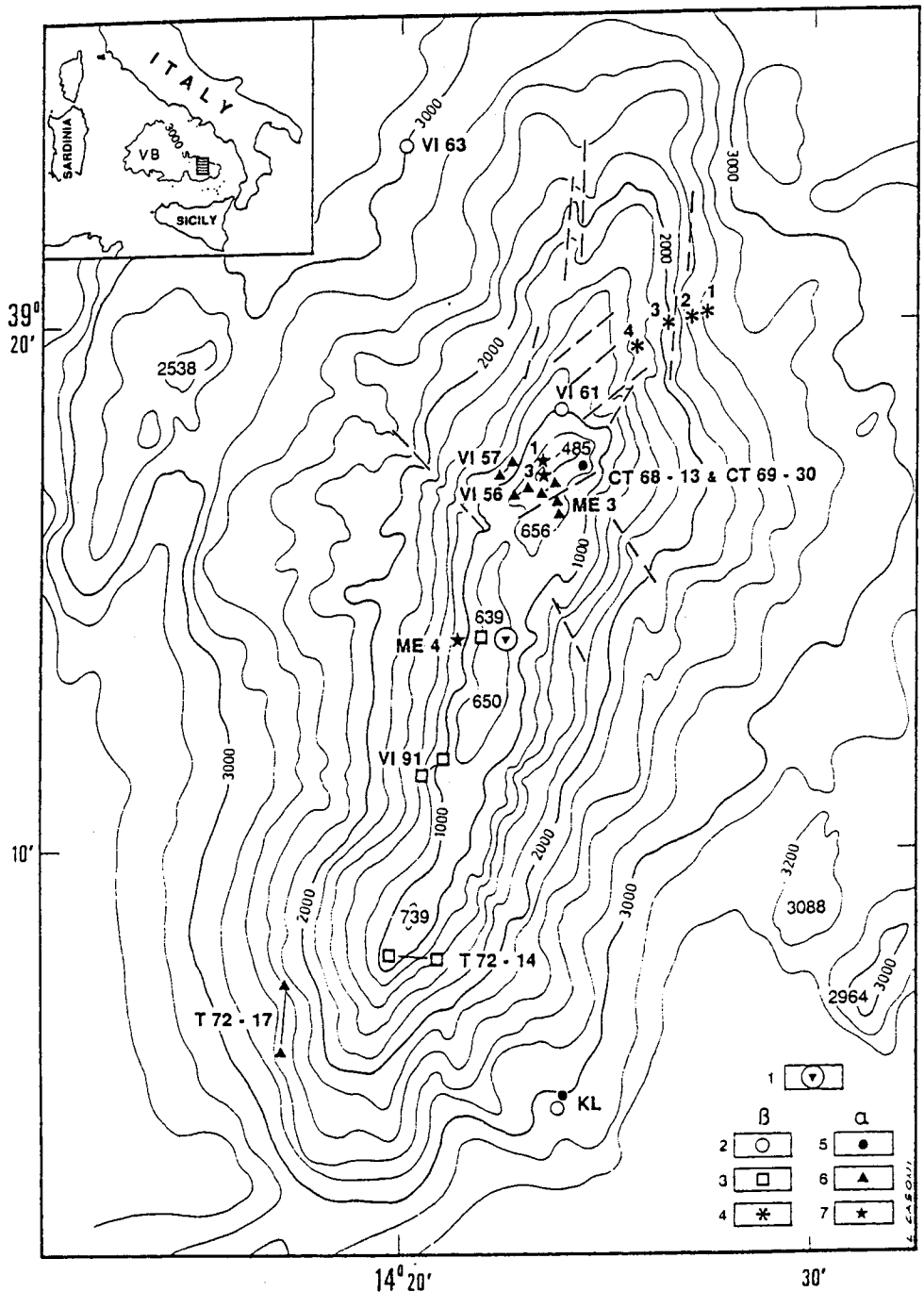

sites: *1* = dredge site of OIB-like basalt (Station CT69/27 of Selli et al., 1977). Lavas of CA affinity: β = basalts, α = andesites; *2* = coring sites of basalt and basaltic andesites; *3* = dredge sites of basalts and basaltic andesites; *4* = sampling sites of basalts recovered during dive no. 21 of the *Mir* 1 submersible; *5* = coring sites of andesites; *6* = dredge sites of andesites; *7* = submersible *Mir* 2 dive no. 16, sampling sites of HKCA andesites (near the top). Dashed lines = fractures in the northern area of seamount; *VB* (inset) = Vavilov Basin.

Fig. 3 Marsili Seamount

3.2. Marsili Seamount

Masili Seamount (Fig. 3) is a 55km long, 25km wide northeast-trending high bordered on its western side by a depression. West of this low are two north-south trending highs with reliefs of 188 and 189m. An echo-sounding survey aboard the R.V. Starella revealed two shallow peaks at the northeast end of the seamount, one at 14°24'10"E, 39°17'14"N with a minimum depth of 490m (uncorrected). The seafloor displays a highly irregular shape made up of numerous mounds, stacks and branch-like structures. The rest of the terrain displayed an earthy-like texture which are typical for manganese oxide or sulphides.

3.3. Aeolian Islands

The Aeolian Islands are located in the geological Southern complex Thyrrenian Sea (Fig. 1), this complexity being demonstrated by the variety of models suggested to explain the geodynamic evolution of the area (Barberi et al., 1974; Scandone, 1979; Ghisetti and Vezzani, 1981; Selli 1981; Boccaletti et al., 1984; Beccaluva et al., 1985; Moussat et al., 1986; Rehault et al., 1987).

Statistical analyses of small- and large-scale deformations on the Aeolian Islands (Frazetta et al., 1982; 1984; Cortese et al., 1986) point to the existence of extensional structures. These occur in two trends which are NE-SW and NW-SE, almost orthogonal to each other. The NW-SE oriented structures, which are probably the surficial expression of a regional deep-seated discontinuity (the Aeolian Islands-Tindari-Girardini-Maltese Escarpment) (Atzore et al., 1978; Carbone et al., 1982), appear to have played a fundamental role in the construction of the Lipari-Vulcano volcanic complexes of the Aeolian archipelago. The evolution of Panarea was, in contrast, mostly controlled by NE-SW trending structures until some point after 25,000 yrs B.P.) (Lanzafame and Rossi, 1984). However, NW-SE structures are also present and are probably still active in Panarea and in the entire archipelago.

The volcanic complex of Panarea (Fig. 4) is shaped like a truncated cone, the edifice rising about 1500m above the seafloor from a lobed base of about 23km in diameter and 460km^2 in area. The volcanic edifice, mainly developed to the east of Panarea, has steep slopes in the eastern sector and a more regular and gentler deeper part. The submarine top is wide and is bounded by a shelf break occurring at an average depth of 120m. This tip is characterized by a complex morphology, featuring depression of varying magnitudes, incisions, and small elevations which culminate in the emerged parts. Many crest lines are radially distributed. The caldera rims identified on Panarea appear to continue partially in the submarine part (Gabbianelli et al., 1990). In this area we also recognized the NE-SW structural trend demonstrated by the elongation of the northeastern margin of the volcanic complex and by the presence of a series of small highs between Panarea and Basiluzzo at minimum dephts of 39-52m. Two other larger structural highs, also occurring along a NE-SW trend, are present at the southeastern end of the complex.

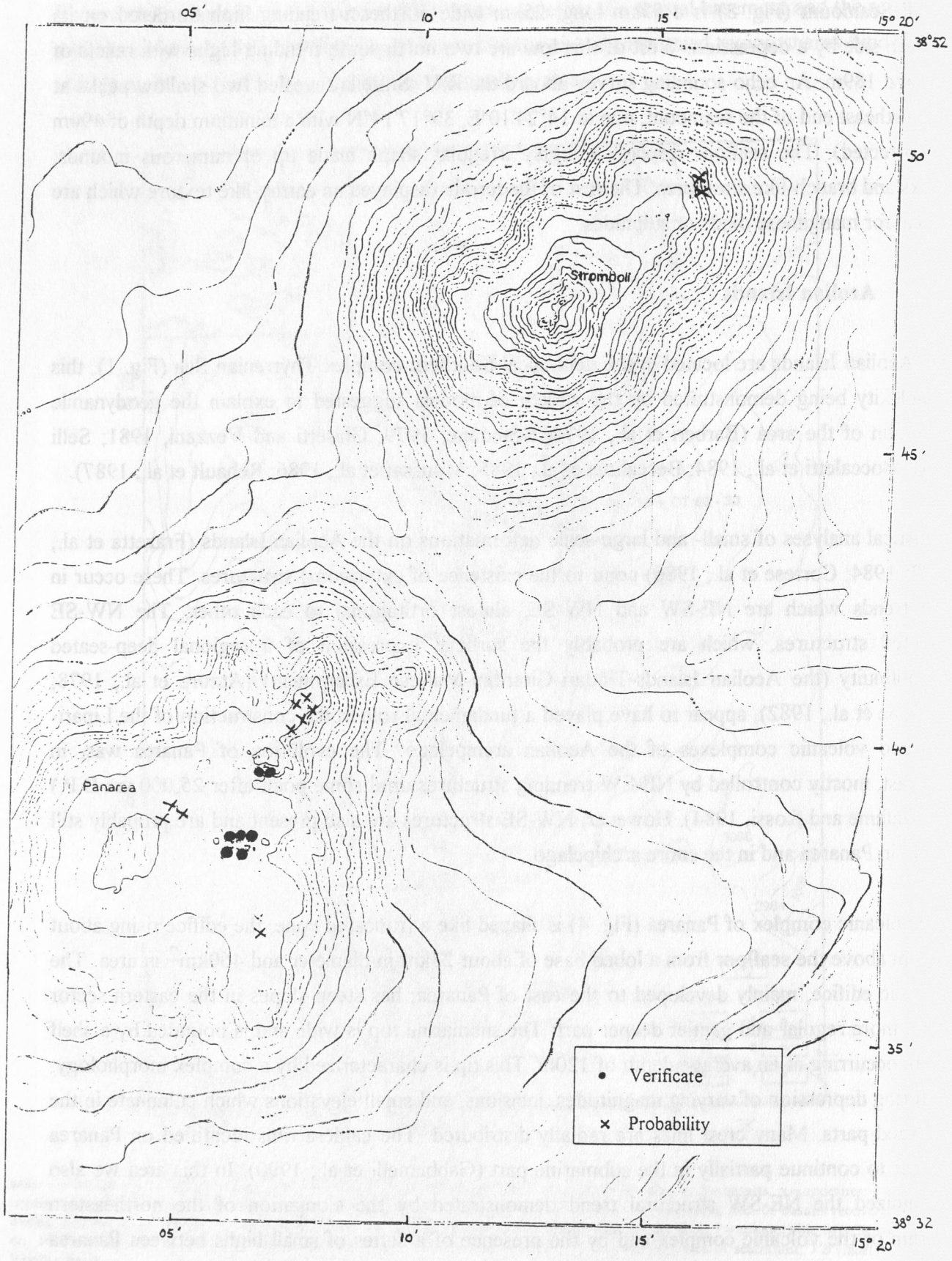

Fig. 4 Southern part of the Aeolian Islands

A shallow (between the depths of 5 and 10m) links Lisca Nera, Bottaro, Panarelli, Lisca Bianca and Dattilo. This is a subcircular structure enclosing a depression reaching 30 m in depth. This depression is probably a crater and includes a highly active large fumarole field, extending along a NE-SW trend, which has caused considerable deposition of whitish sulphur precipitates (Gabbianelli et al., 1990). Other fumarole and/ or hydrothermal phenomena have been detected in the water around Basiluzzo and Panarea (Gabbianelli et al., 1991).

The first results (Lanzafame and Rossi, 1984) indicated that Panarea is the residual part of a large stratovolcano which underwent prolonged evolution and was volcanically and tectonically active up to 25,000 yrs B.P. Fumarole and degassing are still in progress. Particular attention has been given to the importance of the NE-SW-oriented faults in the area. The most recent volcanic phases have been characterized by the emplacement of basaltic scoriae (and therefore by a basic volcanism) never before recognized on the island (Calanchi et al., in press).

The Vulcano island, the southernmost volcanic complex of the Aeolian Archipelago, rises from a continental slope whose complicate morphology is due to the presence of intraslope basins, seamounts, ridges and canyons (Selli, 1974; Savelli and Wezel, 1979; Beccaluva et al., 1981; Gabbianelli et al., 1983). The island is widely described in its general geo-volcanological features (Keller 1980; Frazzetta et al., 1984; Frazzetta and La Volpe, 1987) and many micro- and mesostructural data indicate that the deformations are oriented along two main trends, roughly NW-SE and NE-SW (Frazetta et al., 1982; 1984).

The main volcanic structures (primordial Vulcano, Piano Caldera, fractures of the Piano d'Alighieri, Fossa Caldera and craters) show a time migration from south to north along a NW-SE trend. This trend appears to have played also a fundamental role in the building of the Lipari-Vulcano complex.

The NE-SW tectonic trend is less documented, but very active in the north-central sector of the island. It controls the migration of the eruptive centres of Gran Cratere and Vulcanello (Lo Giudice et al., 1975; Frazzetta et al., 1983) and, probably, also the early fissural activity of Vulcanello.

The limited available information on the submarine portion of the volcanic complex (Belderson et al., 1974; Got et al., 1978) does not allow for the definition of the features of its coastal areas, especially in the zone displaying the most recent volcanic activity.

In recent years the island of Vulcano has recorded a remarkable increase in the fumarolic activity with high variation of its chemical-physical parameters. This has led to more detailed geophysical and geochemical research also aimed at evaluating the volcanic hazard on the island (Budetta et al., 1983; Cioni and D'Amore, 1984; Bonasia et al., 1985; Badalamenti et al., 1986; Carapezza et

al., 1986; Falsaperla and Neri, 1986; Martini 1986; Ferri et al., 1988; CNR-GNV 1988).

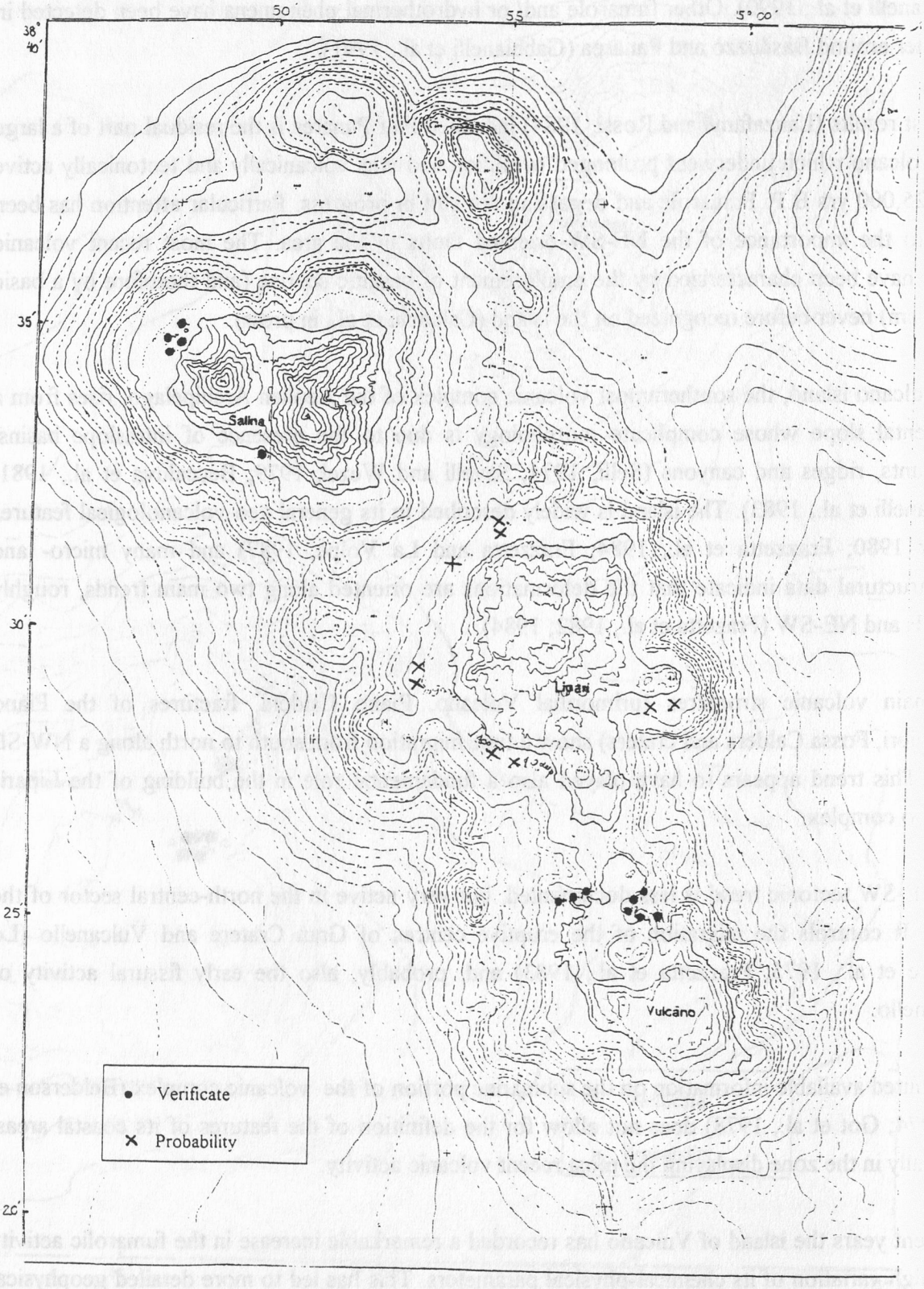

Fig. 5 Northern part of the Aeolian Islands

The eastern flank is characterized by a major morphological uneveness due to the alternation of NE-SW-oriented deep incisions and steep ridges (Gabbianelli et al., 1991). A second isolated relief, never previously detected, is present at the base of the eastern flank at a depth of about -850m (Gabbianelli et al., 1991). Located at 4km east of Punta Luccia, it has a registered minimal depth of -742m and shows a major NE-SW elongation (about 2km in length and 1km in width). The seismic records show the lack of a sedimentary cover and anomalous acoustic responses. These responses are similar to the ones recorded in more surficial areas (Panarea island; Gabbianelli et al., 1991) characterized by exhalative activity (gas and/ or water). Records with similar features were registered also along NE-SW-oriented discontinuities located at the eastern base of the relief (Gabbianelli et al., 1991).

Vulcano Island (Fig. 5), in the Aeolian island arc, north of Sicily, is the emerged part of a 2,000-m-high active volcano built on the Tyrrhenian Sea floor. The Fossa active cone (391m above sea level) was formed in early prehistoric times, in a 2.5-km-wide caldera (Fig. 5). Since its last eruption in 1880-90, it has remained the site of intense fumarolic activity (Sicardi 1941), mainly along the northern edge of the crater. Fumarolic degassing also occurs at and below sea level, along the isthmus connecting the Fossa cone to Vulcanello, a volcanic cone formed by submarine eruptions in 183 BC (Keller 1980). Increasing activity has been observed over the past ten years, especially since 1985. The temperature of the Fossa crater fumaroles rose from 200°C in 1978 (Allard 1978) to nearly 500°C in October 1988 (and > 550°C in July 1989) in connection with an increasing gas outflow, spreading of the fumarolic field and opening of new fractures (Tedesco et al., 1988). Sea-level fumaroles maintain a maximum temperature of 100°C. Their chemical composition is different from that of Fossa cone fumaroles (lack of SO_2, depletion in HCl, enrichment in H_2 and CH_2) (Sicardi 1941; Allard 1978; Carapezza et al., 1981; Cioni and D'Amore, 1984; Martini et al., 1986; Mazor et al., 1988), a feature generally attributed to low-temperature fractionation of the crater-type fluid in shallow aquifers (Carapezza et al., 1981; Cioni and D'Amore, 1984; Martini et al., 1986; Mazor et al., 1988). Isotope data (Polyak et al., 1979); Hooker et al., 1985; Sano et al., 1979) show that both Fossa cone and sea-level fumaroles contain mantle helium, which may derive from a magma intrusion about 1km wide and 2-3km beneath the Fossa crater (Ferrruci et al., 1989). Degassing of this intrusion may thus affect a large area of the island at the surface.

4. Sampling Strategy

Several hydrothermally active spots were known from different literature. The first step of the investigation of hydrothermal areas was to run echosounding profiles across the spot to identify hydrothermal exhalations. Two areas west of Lipari and west of Vulcano could be figured out showing hydrothermal exhalation from the seafloor into the overlying seawater (Fig. 6). The second step was the use of the OFOS system (Ocean floor observation system) equipped with the sensor package and water samplers. The sensor package should measure in-situ hydrothermal

indications in the water column such as Mn, Fe, H_2, H_2S etc. Based on the gradients of the different parameters the OFOS can be used as observation system of the seafloor. While observing hydrothermal exhalation such as shimmering water, fresh hydrothermal precipitates or anomalies of the sensor data, we were able to take water samples from the spot. To get further three-dimensional informations about the overlying seawater, water samples and CTD profiles integrated in a water rosette were taken. Sediment cores were taken from this area to gain information about the underlying sediment.

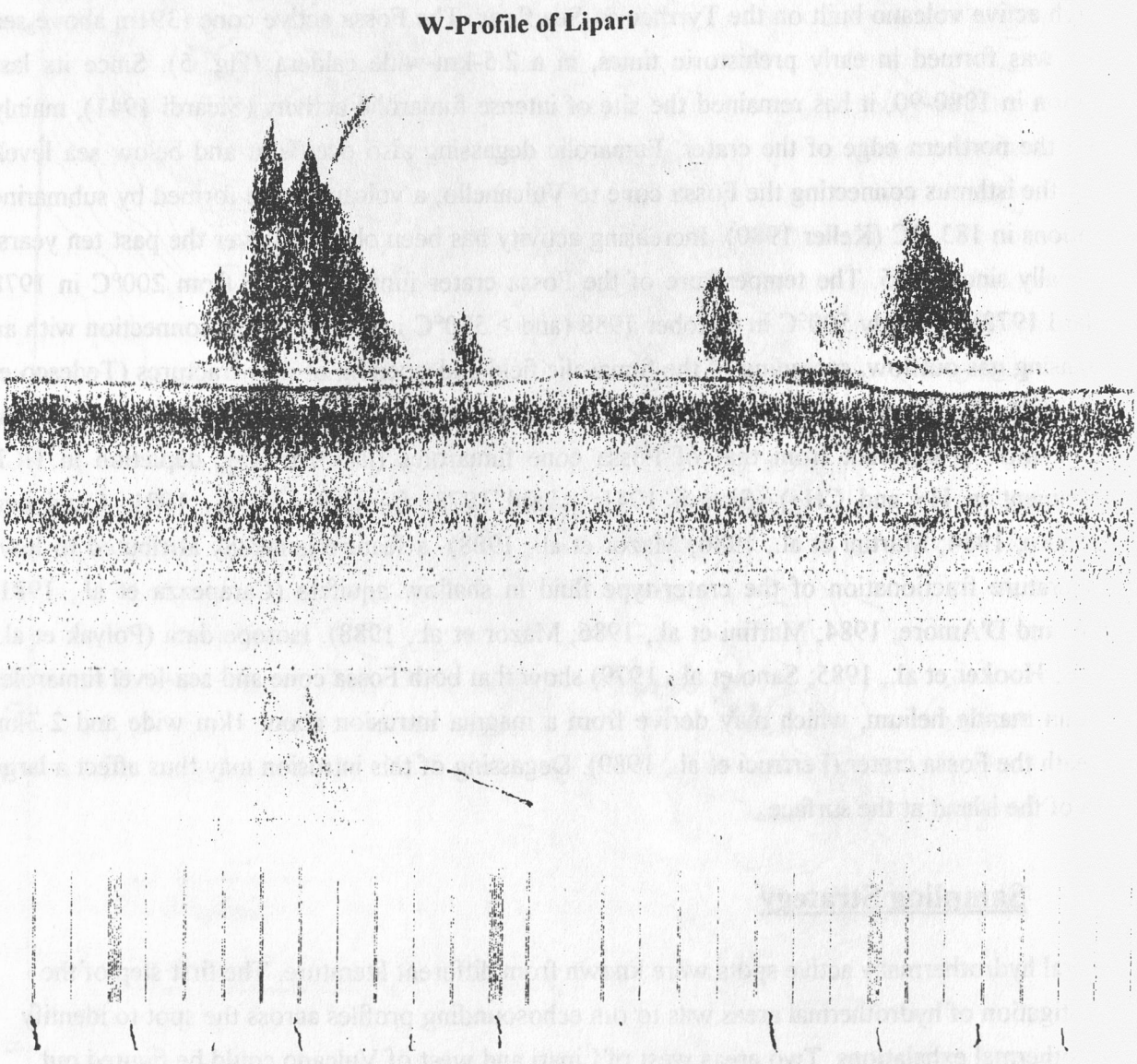

Fig. 6 Echosounding profile W of Lipari

4.1. Water sample collection and processing

4.1.1. Hydrocast samples on Palinuro and Marsili Seamount

Hydrocast water samples were collected in 5l Hydrobios Niskin-type bottles mounted on a rosette equipped with real-time CTD (ADM) above the western-peak of Palinuro seamount (Appendix 2, Stations 340, 346, 353), above the eastern peak of Palinuro seamount (station 362) (Fig. 2). One hydrocast statio was undertaken on top of Marsili seamount (Appendix 2, Station 362) (Fig. 3). Other samples collected in 5l Niskin-type bottles and processed in the same manner as rosette samples were from bottles mounted on the OFOS (Station 354 sample OFOS 354, Station 355 sample OFOS 355 at Palinuro Seamount, and Station 376 sample B-2 at Baziluzzo Seamount, Fig. 2, 5). Other samples are from bottles lowered from an inflatable boat on a kevlar line (Station 370, samples P1-P4 at Panarea, Fig. 4), and from bottles collected on a hydrowire in areas of echo-sounder anomalies (Station 372 samples HC6-1 and HC6-2 at Panarea volcano, and station 377 sample B-4 at Baziluzzo Island, Fig. 4). All samples were immediately processed in the chemistry laboratory of POSEIDON. First, approximately 100ml aliquots were taken for immediate determination of O_2 and pH. Next, aliquots of approximately 60ml were collected without headspace in high-density polyethylene bottles for later determination of chlorinity, and aliquots of around 40ml were syringe-filtered through 0.2 µm-pore Nuclepore filters and frozen in high-density polyethylene bottles for later determination of nutrients (NO_2^-, NO_3^-, NH_4^+, PO_4^{3-} and Si). Finally, 1l subsamples for later determination of trace metals were pressure filtered through a 0.2 µm-pore Nuclepore filter under a glass-100 clean-air bench using filtered nitrogen gas, collected in 1l high-density polyethylene bottles, and acidified with 2ml of concentrated ultrapure HNO_3. No chlorinity or nutrient subsamples were taken from samples HC6-1 and HC6-2. For samples P1-P4, which were collected in an area of probable hydrothermal anomalies, additional subsamples were taken for helium isotopes and CO_2 (cold welded in copper tubes), H_2S (preserved with Zn-acetate in gas-tight glass bottles) and alkalinity (filtered in the same manner as nutrient subsamples, with titrations performed at-sea). Sample processing was completed within 3-4 hours of each hydrocast.

4.1.2. Hydrocast samples at Vulcano island

Shallow vent-water and ambient-water samples were collected from Porto di Levante, Vulcano (Fig. 5), in 1l high-density polyethylene bottles with as little headspace as possible. Ambient water in the bay and fluids over the "hot sands" in the southern part of the bay were collected simply by submerging the bottles, whereas fluids from the vigorously bubbling submarine fumaroles were collected by placing a 19cm-diameter high-density polyethylene funnel over the vent mouth, and collecting the hot fluids through a short length of tygon tubing into 1l high-density polyethylene bottles held above sea level. In all cases, fluid temperatures were measured with a thermometer immediately after filling the sample bottles. Because the vent water contained high concentrations

of dissolved gases, pH and O_2 were measured on-site in fluids collected in glass bottles, and approximately 60ml unfiltered samples were preserved on-site with Zn-acetate in gas-tight glass bottles for later determination of H_2S. Gases from the submarine fumaroles were cold-welded in copper tubes, again using the funnel to allow gases from the vents to pass through tygon tubing and then the copper tubes held above sea level. Water samples were immediately transported to the chemistry laboratory on Poseidon for processing. There aliquots were taken form selected samples for pH measurement, and from each sample, aliquots of around 40ml were syringe-filtered through 0.2 µm-pore Nuclepore filters and frozen in high-density polyethylene bottles for later determination of nutrients. The remaining solutions were pressure filtered through 0.2 µm-pore Nuclepore filters under a class-100 clean-air bench using filtered nitrogen gas and each collected in a 60ml high-density polyethylene bottle. To the 250ml filtered subsamples were added 500 µl of concentrated ultrapure HNO_3 (for later determination of trace metals and minor species); 5ml aliquots from these filtered acidified subsamples were diluted ten-fold with deionized water for later determination of Si. Alkalinity titrations were performed on 25ml aliquots from the 60ml filtered subsamples. Sample processing was completed within 6 hours of sample collection.

4.1.3. Analytical methods

The analytical techniques and estimated analytical uncertainties (in brackets, expressed as percent relative standard deviation on the mean) used to obtain data presented in this report are as follows: Cl^- calculated from chlorinity as determined by $AgNO_3$ titration with colorimetric endpoint (<0.2%); SO_4^{2-} by ion chromatography (<3%); AT by potentiometric titration with HCl against combination pH electrode, calculated with Gran function (<1%; note that thus calculated alkalinities of vent water from Vulcano may require a small correction for high CO_2 content using a modified Gran function); pH by potentiometry with combination pH electrode against NBS buffers (<0.1 pH unit); O_2 by Idronaut polarographic O_2-analyzer (<1%); H_2S by colorimetry with methylene blue method, from ZnS precipitate (<100%); Na^+ by charge-balance calculation of major cations and anions (<0.5%); K^+ by flame atomic absorption spectrophotometry (<5%); Li^+ and Rb^+ by flame atomic emission spectrophotometry using standard additions (<5%); Ca^{2+} by complexiometric EGTA titration with colorimetric endpoint (<0.2%), Mg^{2+} calculated from total alkaline earths as determined by complexometric EDTA titration with colorimetric endpoint (<0.2%); Sr^{2+} by inductively coupled plasma-atomic emission spectroscopy (<10%); dissolved Fe and Mn by flameless atomic absorption spectrophotometry (<15%); Si, NO_3^-, NO_2^-, NH_4^+ and PO_4^{3-} by flow-through colorimetry (<5%).

4.1.4. Results

CTD profiles

The CTD profiles measured on top of the western peak of Palinuro seamount (Appendix 2) show distinct anomaly pattern for the pH value at around 400m water depth in all 4 profiles. There is a steady decrease in pH from the surface to the bottom. An interface layer is obvious at ~ 60m water depth characterized by temperature, conductivity and chlorinity minimum values. There is no further indication of any hydrothermal source from the seafloor at deeper water depths. The CTD profile measured on top of the eastern peak of Palinuro shows a similar pattern (Appendix 2).

The hydrocast station at Marsili seamount shows an interface layer at ~ 120m water depth and no anomalous pH pattern.

The result of the chemical investigations of the different water samples are summarized in Table 1

Table 1: Parameters of the water stations (Pos 200-4)

Station/ Location	Date	Water Depth (m)	Latitude/ Longitude	T (C°)	pH	Cl^-	Eh	O_2 (ppm)	Alca-linity
340	2.5.93	643	39°32'43N	18/16.5	8.1			10.0	-
(HC-1)	"	643	14°42'39E	19.5/19	8.1			10.2	-
W. Pali-	"	643		17	8.1			9.4	-
nuro	"	611		23.5/17	8.1			10.0	-
Summit	"	508		17	8.1			7.7	-
	"	414		17	8.2			10.1	-
346	3.5.93	598	39°32'51N	16.0	8.2			10.1	-
(HC2)	"	590	14°42'26E	17.5	8.2			7.4	-
W. Pali-	"	585		18.0	8.1			7.5	-
nuro	"	509		18.0	8.1			7.5	-
Summit	"	458		19.0	8.1			7.5	-
	"	408		20.5	8.1			7.7	-
	"	433		21.0	8.1			7.6	-
	"	307		20.0	8.1			7.6	-
353	3.5.93	647	39°31'39N	16.0	8.2			8.0	-
(HC3)	"	640	14°42'37E	17.5	8.1			7.9	-
W. Pali-	"	635		18.5	8.1			7.9	-
nuro	"	625		18.0	8.1			7.9	-
Summit	"	595		19.0	8.1			7.9	-
	"	305		19.5	8.1			7.8	-
	"	504		19.5	8.1			7.6	-
	"	403		19.5	8.1			7.8	-
354	4.5.93	see	39°32'48N	17.5	8.2		158	7.8	-
OFOS-		OFOS	14°42'16E						-
sensors		records							-

Station/ Location	Date	Water Depth	Latitude/ Longitude	T (C°)	pH ()	Cl^-	Eh ()	O_2 (ppm)	Alca-linity
355	"	see	39°31'33N	20-0	8.2		184	8.9	-
OFOS-		OFOS-	14°39'64E						-
sensors		records							-
(P.S.)									
									-
356	"	783	39°31'30N	17.0	8.1			8.3	-
(HC4)	"	777	14°39'50E	18.0	8.1			7.9	-
E. Palinuro	"	772		18.5	8.1			8.0	-
Summit	"	762		19.0	8.1			7.9	-
	"	742		20.0	8.1			9.5	-
	"	510		20.0	8.1			7.8	-
	"	662		20.5	8.1			7.9	-
	"	408		20.5	8.1			9.1	-
	"	545							
362	6.5.93	667	39°17'02N	16.0	8.2			8.0	-
(HC5)	"	661	14°23`65E	17.0	8.2			10.0	-
Marsilli	"	656		18.5	8.1			9.9	-
Summit	"	646		19.0	8.1			8.2	-
	"	625		18.5	8.1			8.1	-
	"	506		19.5	8.1			9.7	-
	"	431		19.0	8.1			8.1	-
	"	356		19.5	8.1			8.0	-
370	8.5.93	ca. 27	38°38'30N	18.5	8.2				2.62
(Rubber	"	ca. 22	15°06'30E	19.0	7.9			9.5	2.60
boat)	"	ca. 17		22.0	8.2			8.9	2.55
Niskins	"	ca. 27		19.5	8.2			9.3	2.62
Near									
Panarkea									
372	"	ca. 65	38°39'97N	17.0	8.2			9.0	-
(HC6)	"	ca. 60	15°06'04E	17.5	8.1			9.1	-
Near									
Basiluzzo									
376	9.5.93		38°30'63N						
(OFOS)		115	14°53'64E	19.0	8.2			9.5	-
Near									
Basiluzzo									
377	"		38°31'3N						
(Hydrowire)		ca. 92	14°54'3E	20.0	8.2			8.6	-
Near									
Basiluzzo									

Vulcano fluids

Si and T: Si as a normalizing variable

All of the warm fluid samples collected from Porto di Levante are highly enriched in dissolved Si relative to "ambient" bay water (47-88 µmol/kg Si), reaching 1630 µmol/kg Si in a 65.5°C sample from the beach-fumarole site. The Si vs T data for the beach-fumarole samples define a single straight line within the uncertainty of the temperature measurements (around± 5°C) measurements, whereas the three data points from the hot-sand site define a steeper Si vs T relationship (Fig. 7). The simplest interpretation of the beach-fumarole Si-T trend is that the data define a mixing line between the warm Si-rich fluids and ambient bay water, with dissolved Si behaving approximately conservatively during this process, as observed for other submarine warm springs (e.g., EDMOND et al., 1979; SEDWICK et al., 1992). Thus, dissolved Si concentration can be used as a mixing tracer for these samples to examine the mixing trends of other species. Although samples from the hot-sand site are too limited to determine whether a linear Si vs T trend exists, a linear relationship (with a greater Si/T ratio than for the beach-fumarole fluids) is assumed.

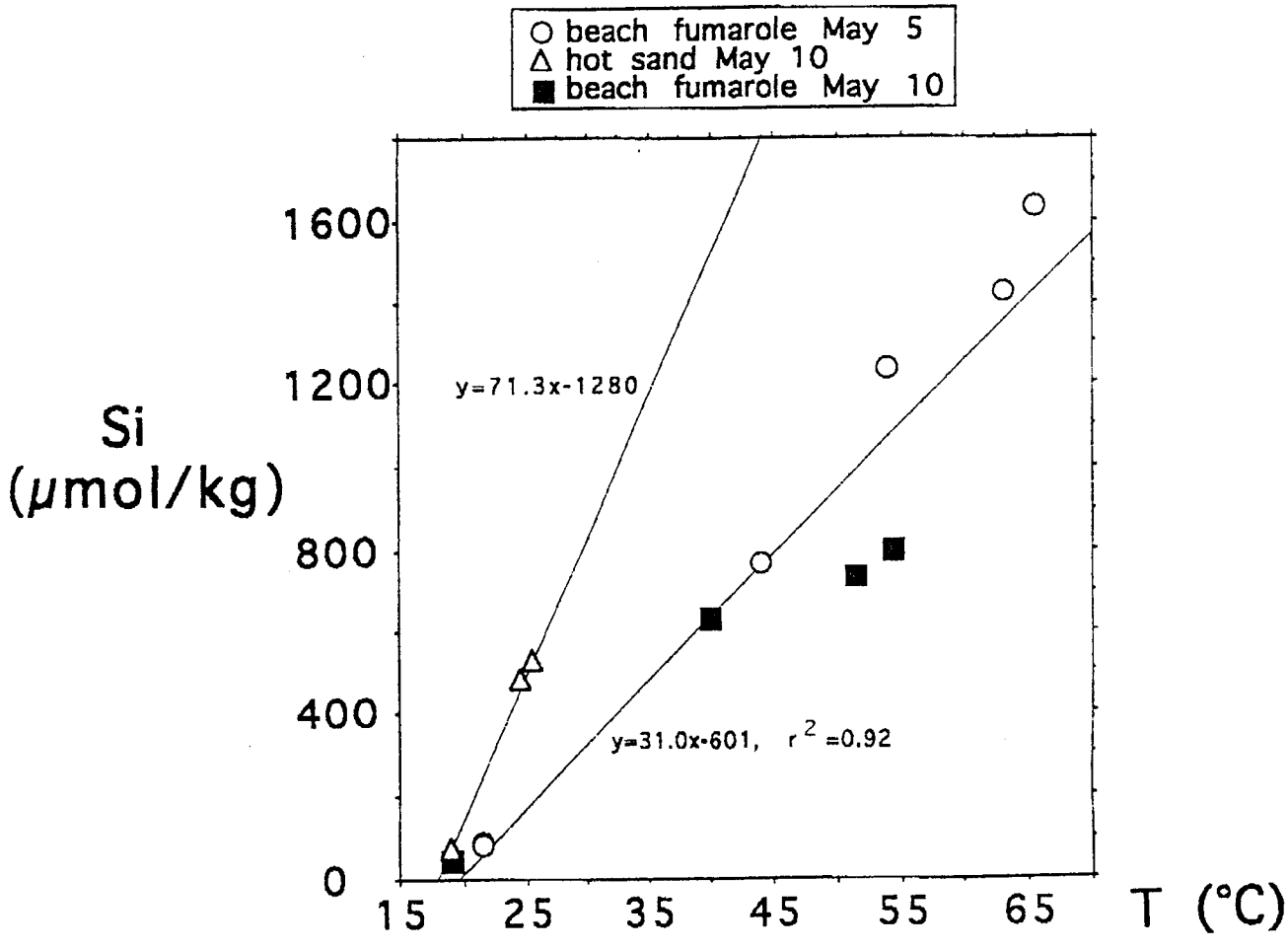

Figure 7: Chemical composition of vent water sampled in the coastal area of Vulcano - Temperature versus Si content

Dissolved gases (O_2 and H_2S) and pH

Hydrogen sulfide was smelled throughout the embayment, particularly around the beach-fumarole site. A sample of "ambient" bay water contained 153 µmol/kg H_2S (much higher than the sub-micromolar concentrations typical of oxygenated seawater), whereas two fluid samples taken from the beach-fumarole site contained 273 and 166 µmol/kg H_2S. No H_2S samples were collected from the hot-sand site, although the warm fluids collected there also smelled of H_2S. Vent fluids from the beach fumarole site are clearly depleted in dissolved oxygen relative to ambient bay water (0.28 mmol/kg O_2), with field measurements indicating 0.04 and 0.11mmol/kg O_2 respectively. No dissolved O_2 measurements were made for fluids from the hot-sand site. The pH vs Si data in Figure 8 (pH measured in the laboratory) show that the warm fluids from the beach-fumarole site and the hot-sand site are quite acidic (pH 5.5-6.3) relative to ambient samples at both sites (pH 6.5-7.5), with field pH measurements suggesting even lower values (ambient bay water pH ~ 6.1, beach-fumarole fluid pH ~ 5.2-5.4).

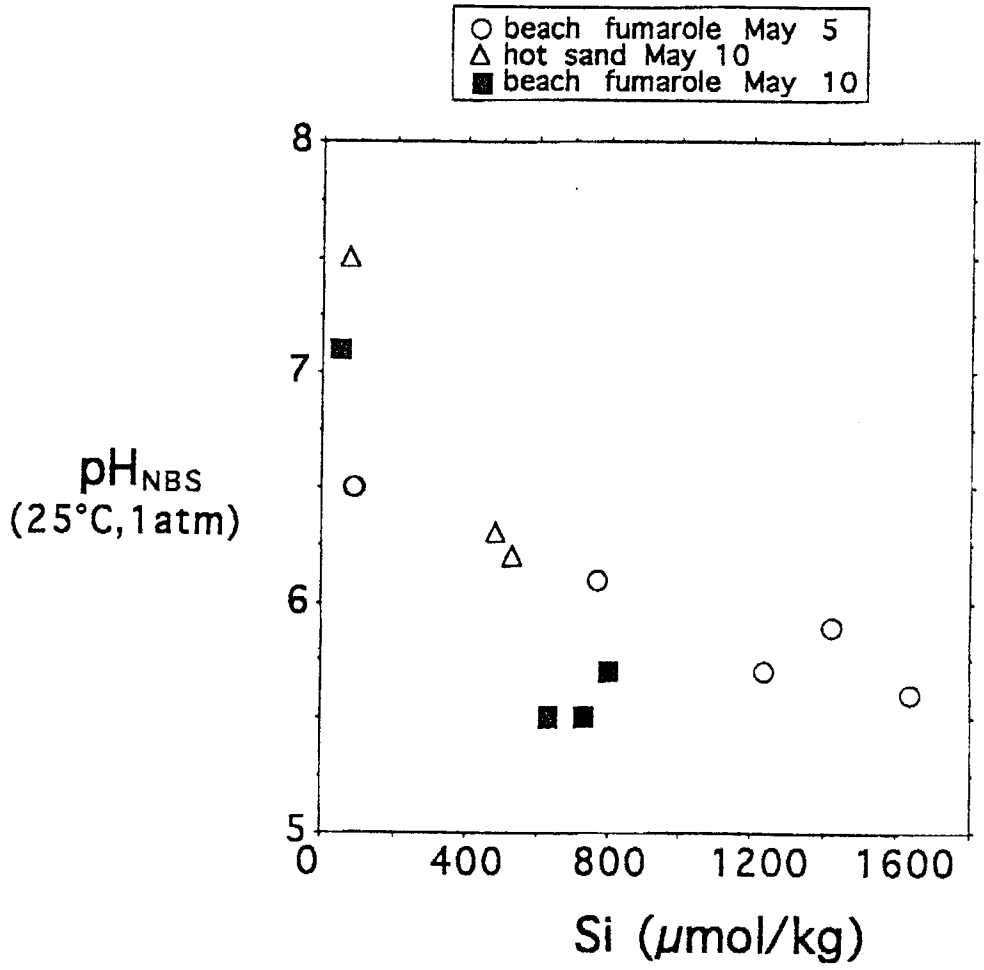

Figure 8: pH versus Si content

The anions: Cl^-, SO_4^{2-} and A_T

For samples from the beach-fumarole site, dissolved Cl^- is depleted by more than 6% relative to ambient bay water and negatively correlated with Si, although there are apparently different mixing trends for the two sampling dates (Fig 9). The two warm samples from the hot-sand site are also slightly depleted in Cl^-, although observed depletions are close to the analytical uncertainty. The low chlorinity of the beach-fumarole fluids relative to seawater may reflect introduction of low-salinity groundwater in the subseafloor, or is more likely a result of phase separation and subsequent phase segregation of seawater during hydrothermal alteration, given the near-boiling temperature of the vented fluid. To a first approximation, both of these processes may be assumed equivalent to dilution of the altered seawater by deionized water, and a correction made for the effect of either processe on the fluid compositions by normalizing the concentration data with respect to the chlorininty of ambient bay water. Titration alkalinities of the warm fluids are depleted over ambient bay water by over 20%, and negatively correlated with dissolved Si for the three sample sets (Fig. 10a); the data trends are little changed by normalizing A_T with respect to ambient chlorinity (data not shown). The SO_4^{2-} data show no trend versus Si for the three sample sets within the analytical uncertainty (Fig. 10b); there remains no discernable trend if the SO_4^{2-} data are normalized with respect to ambient chlorinity (data not shown).

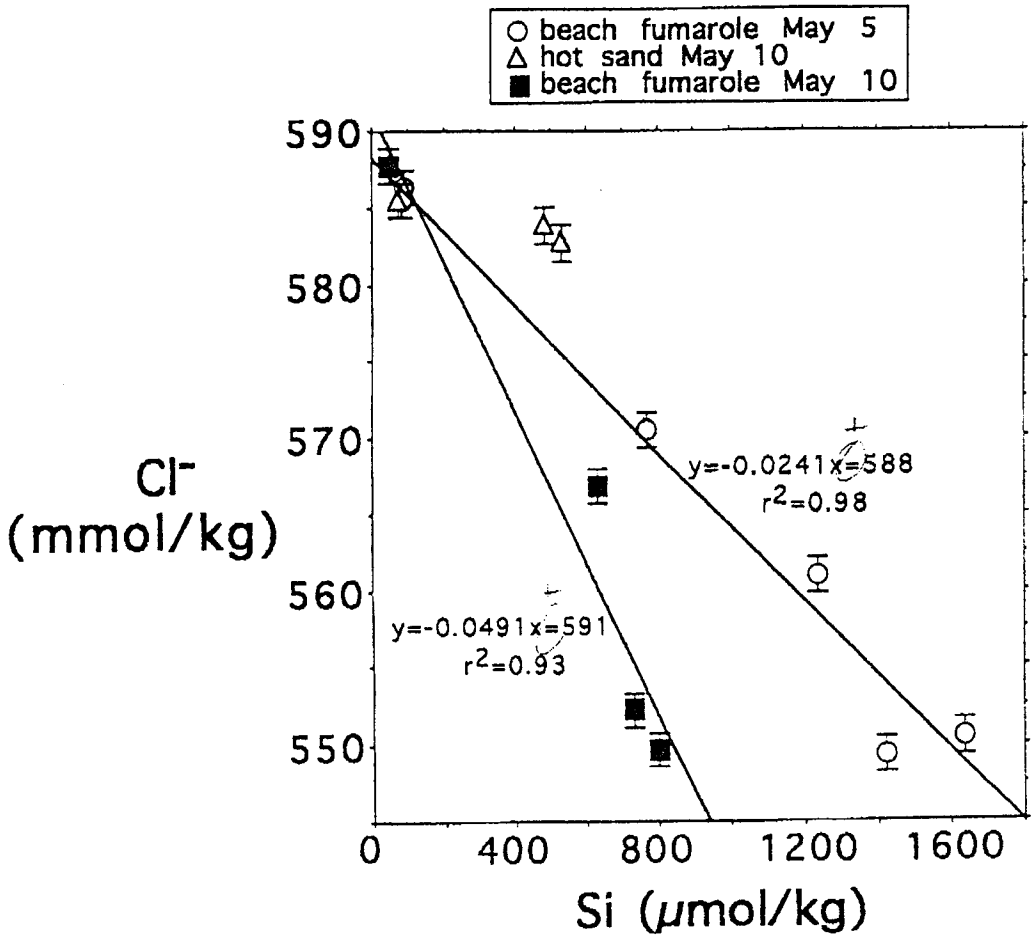

Figure 9: Chlorid versus Si content

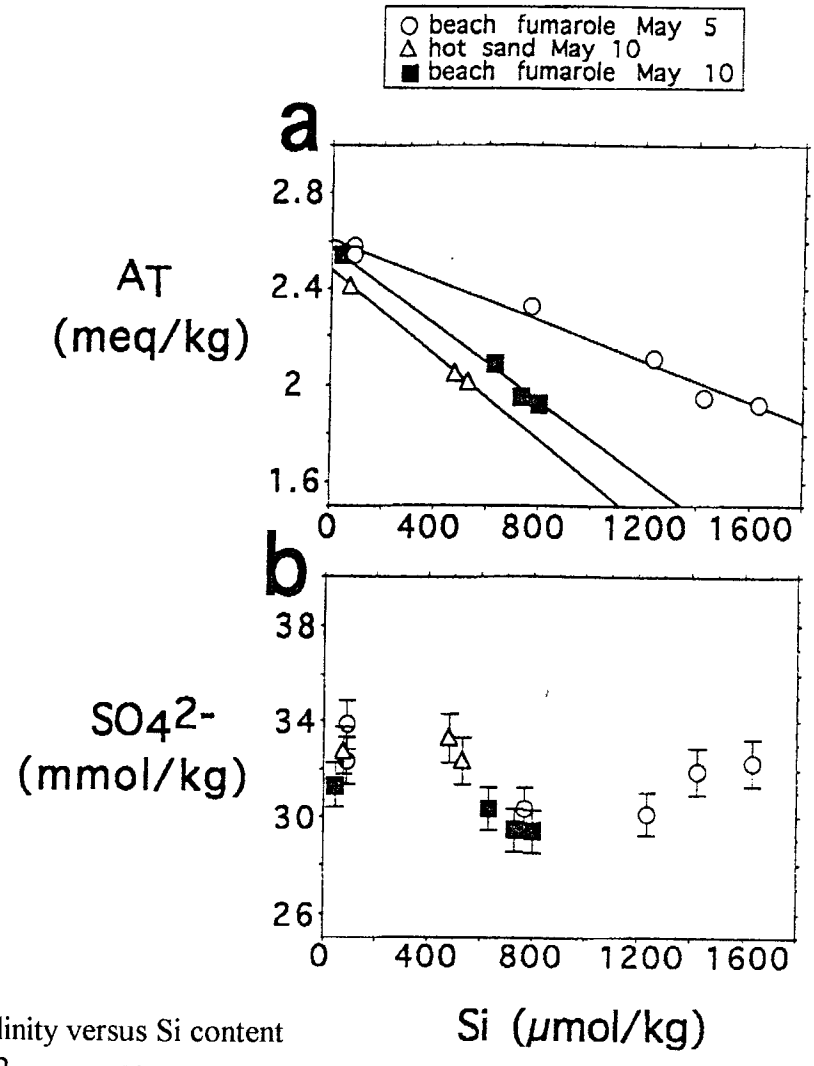

Figure 10: a Alcalinity versus Si content
b SO_4^{2-} versus Si content

The alkali metals: Na^+, K^+, Li^+ and Rb^+

The Na^+ (calculated by charge balance) concentrations of the beach-fumarole and hot-sand fluids are lower than ambient bay water (Fig. 11a); however, the Cl-normalised Na^+ data show no depletion, suggesting that the apparent Na^+ depletions reflect only the lower salinity of the warm fluids (Fig. 11b). The dissolved K^+ data show no clear trend versus Si within the analytical uncertainty (Figs. 11c), although the Cl-normalized data suggest a slight enrichment of the May 5 beach-fumarole samples and hot-sand samples relative to ambient concentrations (Fig. 11d). Dissolved Li^+ and Rb^+ are both significantly enriched over ambient bay water in the beach-fumarole fluids (by over 50% and 250%, respectively) and the hot-sand fluids (by over 80% and 200%, respectively); both species correlate highly with Si, with indistinguishable trends (within error) for the two beach-fumarole (Figs. 12a,b). Normalising the Li^+ and Rb^+ concentrations with respect to chlorinity has little effect on the data trends (data not shown).

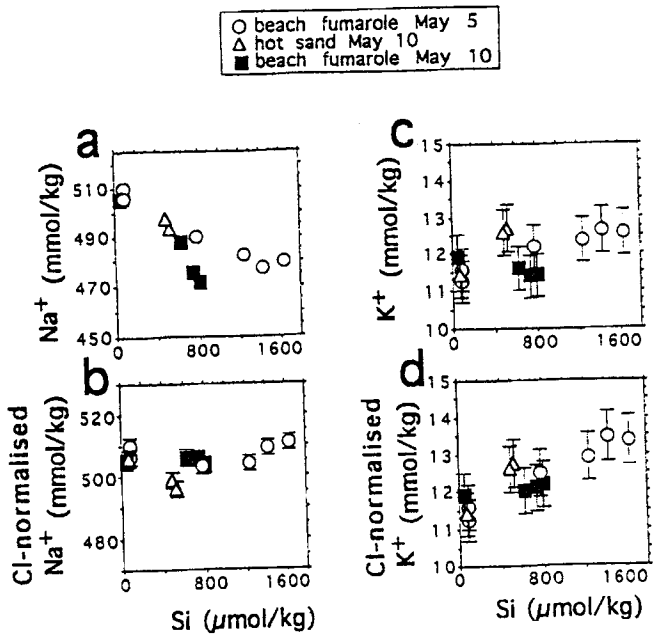

Figure 11 a: Na^+ versus Si, b: Cl-norm Na versus Si, c: K^+ versus Si, d: Cl-norm K^+ versus Si

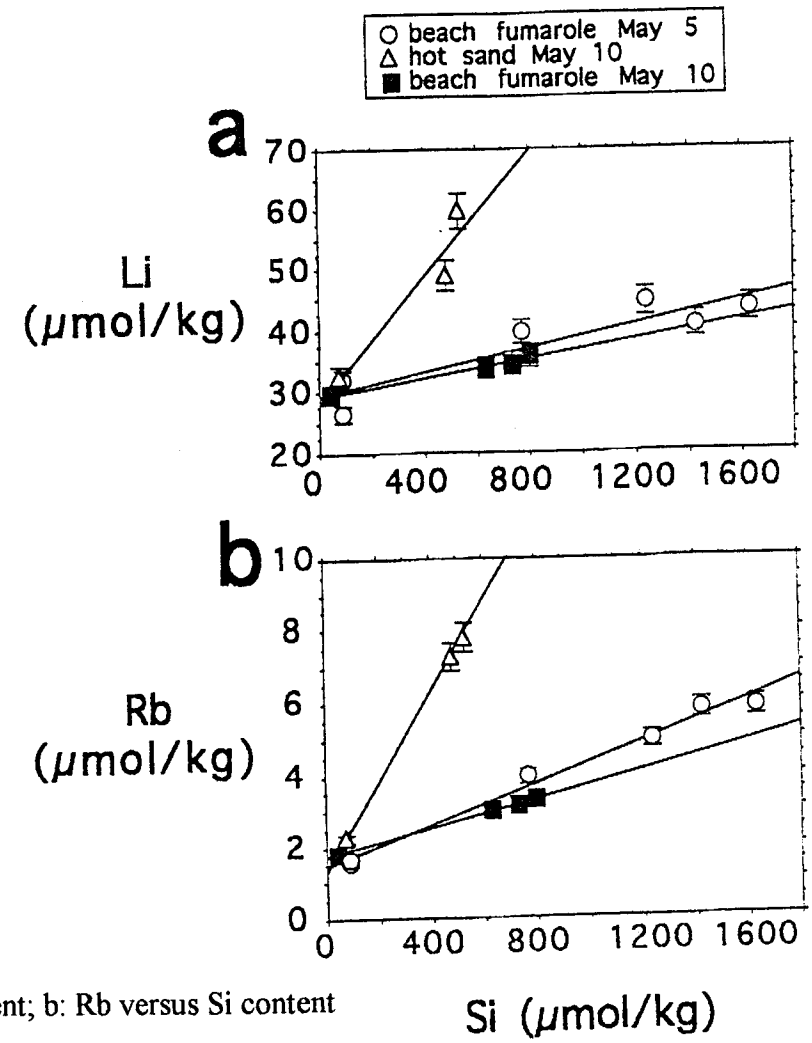

Figure 12: a: Li versus Si content; b: Rb versus Si content

The alkaline earths: Mg^{2+}, Ca^{2+} and Sr^{2+}

The beach-fumarole fluids are depleted in Mg^{2+} by nearly 10% relative to ambient bay waters (Fig 13a); correcting for the "diluting" effect of the low-chlorinity hot fluids by normalising with respect to chloride reduces this depletion to ~2% for the May 5 samples and eliminates any clear mixing trend for the May 10 data. The Mg-depletion of the May 5 samples likely reflects removal of Mg from the starting seawater during hydrothermal alteration, which is thought to be quantitative at 70°C (or even lower temperatures) during reaction of seawater with basalt (MOTTL, 1983). In other studies of submarine hydrothermal fluids where water samples are thought to represent mixing of a Mg-free hydrothermal endmember fluid with seawater, the temperature of the hydrothermal endmember has been estimated by extrapolating data to the temperature of zero-Mg (e.g., see EDMOND et al., 1979). Performing this calculation for the raw Mg data for the beach-fumarole samples yields zero-Mg at 18.8 and 10.1 mmol/kg Si for the May 5 and May 10 samples, respectively. The Si vs T relationship of Figure 7 then yields zero-Mg temperatures of 626°C and 345°C respectively, and much higher temperatures if the Cl-normalised Mg data are used. Performing this same exercise directly for the Mg versus T data (Figs 14a,b) yields similar zero-Mg temperatures. Noteably, the two warm samples from the hot-sand site are *enriched* in Mg by several percent relative to ambient, a situation generally *atypical* for seawater-derived hydrothermal fluids.

Dissolved Ca^{2+} is slightly (up to ~7%) depleted over ambient bay water in the beach-fumarole samples, and significantly enriched (up to ~16%) in the hot-sand samples (Fig. 15a) However, Cl-normalising these data to remove the dilution effect of the low-chlorinity fluids shows no trend for the May 5 beach-fumarole samples and a slight Ca^{2+} enrichment for the May 10 beach fumarole samples; the trend for the hot-sand samples remains unchanged (Fig. 15b). The Sr^{2+} versus Si data suggest a depletion in the beach-fumarole fluids relative to ambient bay water, however the apparent depletions are within the analytical uncertainty of the Sr^{2+} determinations (Figs. 15,d).

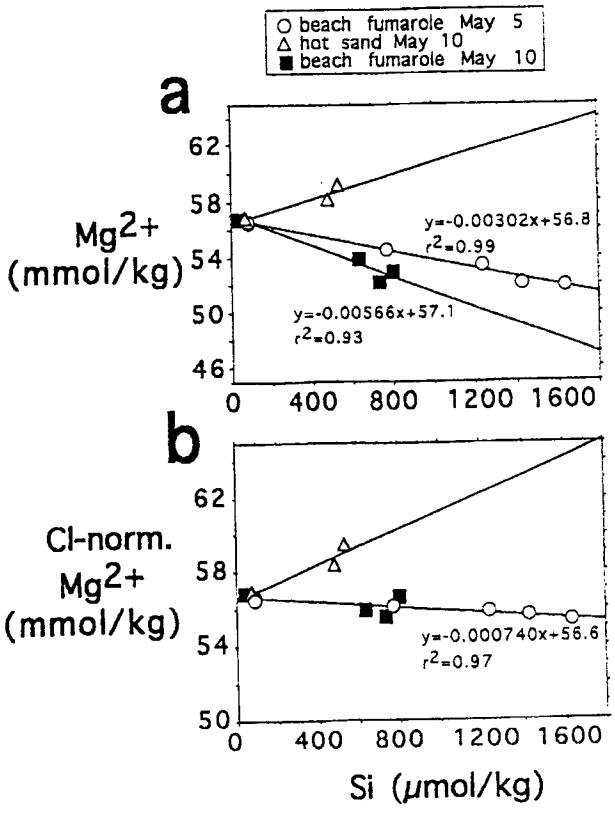

Figure 13 a: Mg^{2+} versus Si content

b: Cl-norm. Mg^{2+} versus Si content

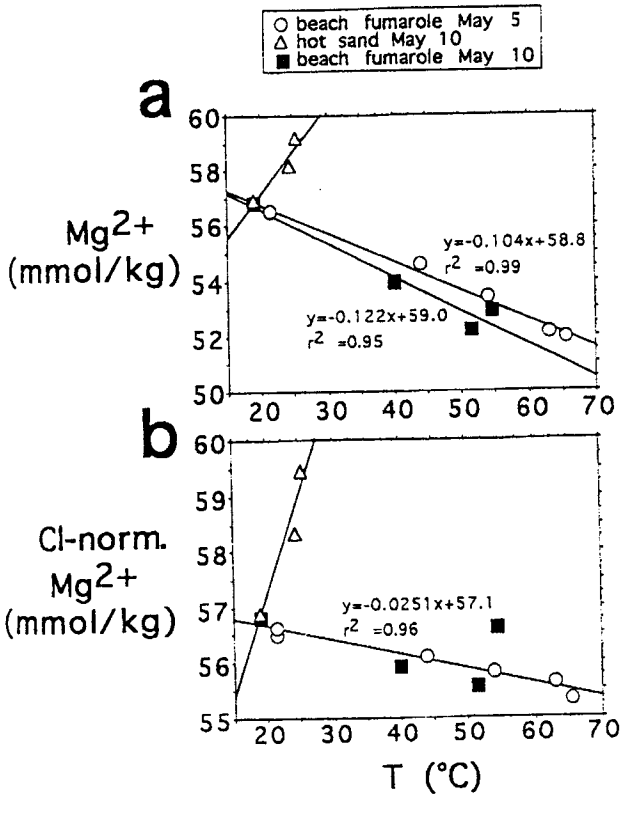

Figure 14: a: Mg^{2+} versus T

b: Mg^{2+} versus T

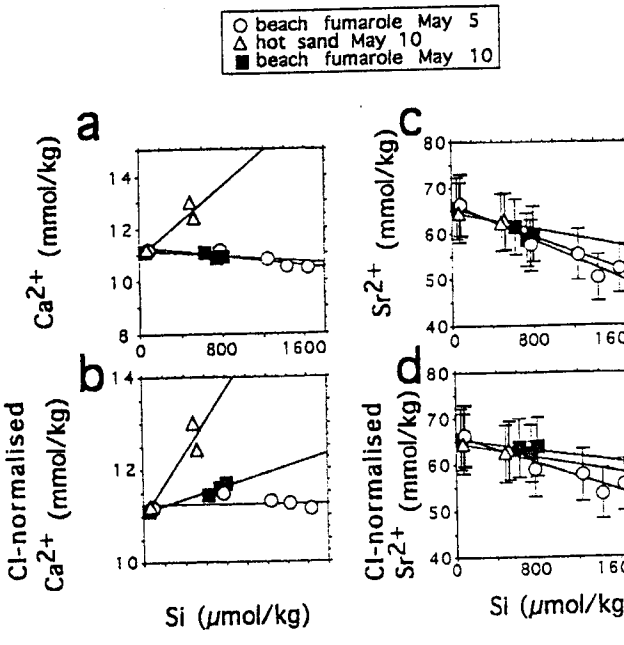

Figure 15: a: Ca^{2+} vs Si

b: Cl-norm Ca^{2+} vs Si

c: Sr^{2+} vs Si

d: Cl-norm. Sr^{2+} vs Si

The transition metals: Fe and Mn

Dissolved Fe is enriched by almost an order of magnitude over ambient values in the beach-fumarole samples, and is highly enriched (by more than 100x) in the hot-sand samples (Fig 16a). Dissolved Mn is also enriched by around an order of magnitude relative to ambient concentrations in both the beach-fumarole and hot-sand fluids, and correlates highly with Si (Fig. 16b). Normalising the Fe and Mn data with respect to chloride (data not shown) does not significantly affect the observed trends.

The nutrients: NO_3^-, NO_2^-, NH_4^+ and PO_4^{3-}

Dissolved $NO_3^-+NO_2^-$ concentrations, as well as NO_3^- and NO_2^- concentrations alone, show no consistent trend against dissolved Si (Fig. 17a). In the beach-fumarole samples, NH_4^+ is significantly enriched (up to ~30x) over ambient bay water and highly correlated with Si, whereas no trend is discernable for the hot-sand samples (Fig. 17b); notably, the NH_4^+ concentrations of the beach-fumarole fluids are far in excess of that which could be supplied by reduction of NO_3^- and NO_2^- from ambient seawater. The PO_4^{3-} vs Si data for the beach-fumarole samples suggest that these fluids are enriched in PO_4^{3-} relative to ambient seawater, although fluid concentrations from the hot-sand site are uniformly low (Fig. 17c). Some of the scatter in the $NO_3^-+NO_2^-$ and PO_4^{3-} data may reflect biological processes occuring after sample collection, given the abundant bacterial mats surrounding the beach fumaroles.

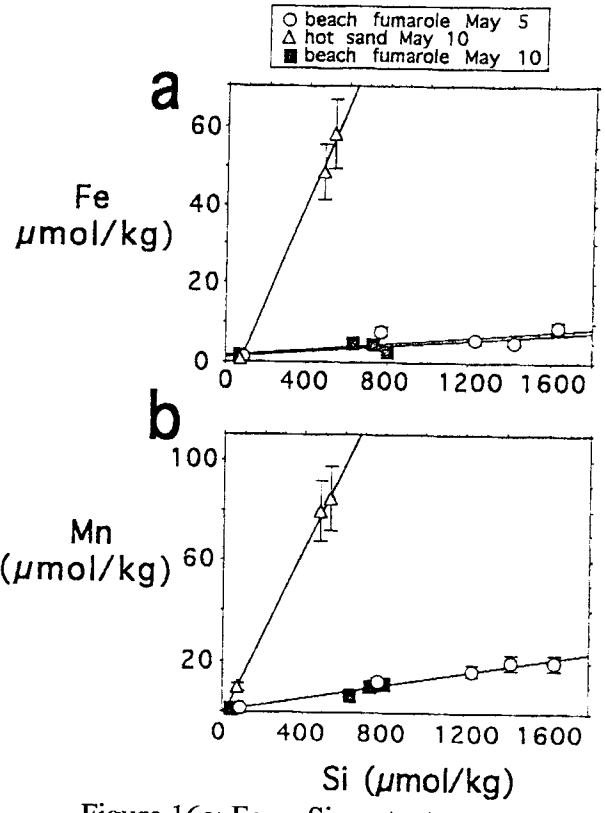

Figure 16a: Fe vs Si content

b: Mn vs Si content

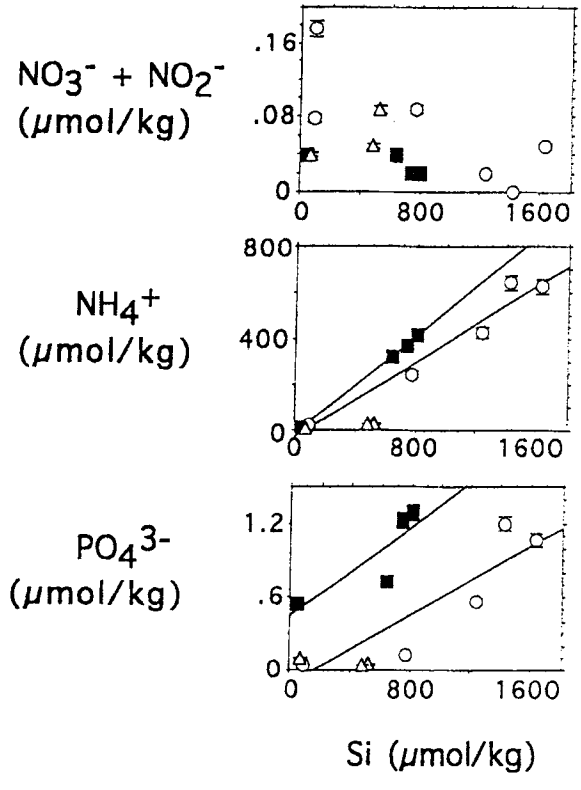

Figure 17a: $NO_3^-+NO_2^-$ vs Si

b: NH_4^+ vs Si

c: PO_4^{3-} vs Si

Palinuro

The results of the chemical composition of the water samples are summarized in Table 2 and 3. In the investigated E-peak of Palinuro volcano the samples seawater has significant Mn concentrations, reaching maximum values of 1.38 ppb (Fig. 18). On the Palinuro W peak a maximum Mn content of 0.1 ppb has been found. Also the Mn contents of water sampled above the Marsili are higher (up to 0.41 ppb of Mn) than normal seawater values which range from 0.02 to 0.06 ppb of Mn.

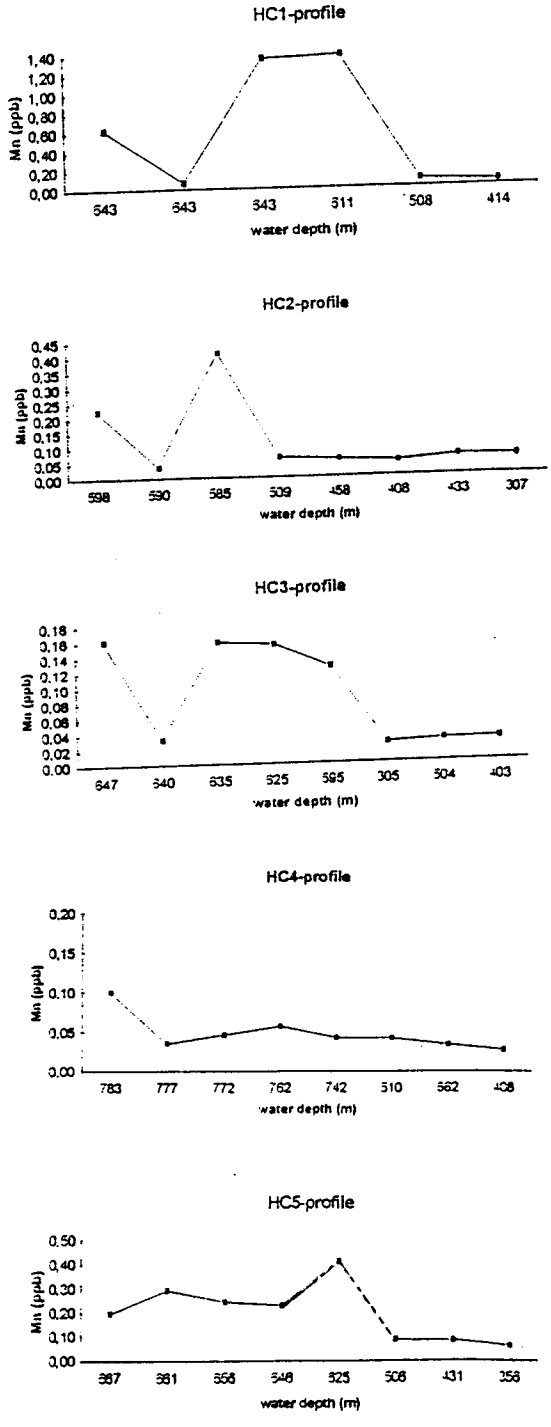

Fig. 18 Mn concentrations of the different stations

Table 2

Nutrient concentrations (ppm) in water samples of the 200/4 cruise

Probe	NO_2	SiO_2	NH_4	NO_3	PO_4
HC1-1	0.01	7.71	0.23	6.02	0.27
HC1-2	0.00	5.89	0.60	5.66	0.24
HC1-3	0.01	7.55	0.26	6.03	0.27
HC1-4	0.01	7.43	0.22	6.37	0.27
HC1-5	0.00	6.81	0.14	5.83	0.27
HC1-6	0.01	6.46	0.08	5.70	0.26
HC2-1	0.01	7.48	0.10	6.16	0.26
HC2-2	0.00	6.39	0.26	6.31	0.25
HC2-3	0.00	8.10	0.07	6.75	0.26
HC2-4	0.00	7.17	0.11	6.31	0.26
HC2-5	0.01	6.84	0.01	5.99	0.25
HC2-7	0.31	6.86	0.45	7.18	0.25
HC2-8	0.01	6.84	0.12	5.90	0.25
HC3-1	0.01	8.34	0.03	6.24	0.27
HC3-2	0.01	5.81	0.11	5.56	0.23
HC3-3	0.00	8.24	0.02	6.22	0.25
HC3-4	0.00	8.16	0.03	6.17	0.25
HC3-5	0.00	8.22	0.00	6.20	0.26
HC3-6	0.00	7.96	0.00	5.79	0.23
HC3-7	0.00	7.70	0.04	5.69	0.24
HC3-8	0.00	7.75	0.11	5.79	0.24
HC4-1	0.00	7.90	0.11	6.24	0.20
HC4-2	0.00	6.76	0.06	6.03	0.20
HC4-3	0.00	7.51	0.00	6.13	0.20
HC4-4	0.00	7.77	0.01	6.12	0.22
HC4-5	0.00	7.96	0.17	6.08	0.21
HC4-6	0.01	7.89	0.11	6.11	0.20
HC4-7	0.00	7.17	0.09	5.83	0.20
HC4-8	0.00	8.38	0.10	6.08	0.22
HC5-1	0.01	8.85	0.09	30.5	0.23
HC5-2	0.00	8.50	0.14	6.47	0.22
HC5-3	0.01	9.01	0.11	6.47	0.22
HC5-4	0.01	9.08	0.14	6.50	0.23
HC5-5	0.01	9.28	0.05	6.87	0.23
HC5-6	0.01	8.51	0.11	6.14	0.22
HC5-7	0.01	8.16	0.15	5.97	0.22
HC5-8	0.01	8.92	0.10	6.05	0.22
P1	0.02	3.08	0.23	0.18	0.04
P2	0.01	4.52	0.22	0.00	0.04
P3	0.01	7.71	0.13	0.01	0.03
P4	0.01	3.57	0.26	0.17	0.07
OFOS	0.02	0.00	0.28	0.00	0.15
OFO-PAL	0.01	6.60	0.00	6.23	0.23
204 B2	0.05	0.85	0.07	1.20	0.07
204 B4	0.05	0.72	0.15	0.94	0.05

Table 3a: Mn, Fe concentrations in water samples of the Pos 200-4 cruise

Sample No.	Fe (ppb)	Mn (ppb)
V 1	68.2	72.1
V 2	74.1	74.3
V 3	510.0	1117.5
V 4	305.0	1122.5
V 5	330.0	929.3
V 6	453.0	674.4
V 7	3320.0	4768.0
V 8	2759.0	4479.3
V 9	29.6	544.4
V 10	284.0	358.9
V 11	152.0	631.3
V 17	267.0	559.9
V 18	3202.0	43.9
P 1	<5	<5
P 2	<5	24.9
P 3	<5	<5
P 4	<5	<5
HC 6-1	<5	<5
HC 6-4	<5	<5
B 2	<5	<5
B 4	<5	<5

Table 3b: Mn, Fe concentrations in water samples of the Pos 200-4 cruise

Sample	Mn (ppm)	Sample	Mn (ppm)
HC1-1	0.6241	HC4-1	0.0997
HC1-2	0.0654	HC4-2	0.0352
HC1-3	1.3	HC4-3	0.0463
HC1-4	1.3	HC4-4	0.0573
HC1-5	0.0787	HC4-5	0.0424
HC1-6	0.0482	HC4-6	0.0425
		HC4-7	0.0341
HC2-1	0.2229	HC4-8	0.0272
HC2-2	0.0359	HC5-1	0.1956
HC2-3	0.4104	HC5-2	0.2944
HC2-4	0.0647	HC5-3	0.2473
HC2-5	0.0561	HC5-4	0.2303
HC2-6	0.0479	HC5-5	0.4134
HC2-8	0.0607	HC5-6	0.0884
		HC5-7	0.0839
HC3-1	0.161	HC5-8	0.0612
HC3-2	0.0327	OFOS 354	0.4007
HC3-3	0.1586	OFOS 355	0.2134
HC3-4	0.1550		
HC3-7	0.0288		
HC3-8	0.0293		

4.2. Seafloor observation and sediment coring

On Palinuro seamount three OFOS runs (Stat. 339, 354, 357) have been undertaken within a Transponder navigation array (Fig. 19). On top of Marsili seamount the seafloor was observed and characterized during one OFOS run (Stat. 366). Two OFOS profiles have been done in the area of Lipari (Stat. 375, 376) and one at Panarea, Baziluzzo (Stat. 370).

The seafloor observation was made with the Ocean Floor Observation system - OFOS, equipped with black and white TV and photo cameras, and towed at an elevation around 5 m above the seafloor at a ship`s speed of half a knot.

Near the two sulfide outcrops of Palinuro seamount (Fig. 2), one at 39°32.18N and 14°42.37E at 685 m water depth (Puchelt and Laschek, 1986), the other at 39°31.22N and 14°39.70E at 675 m (Minniti and Bonavia, 1984), some of the seafloor pictures suggest turbid water shimmering above dark gray sediment (Fig. 20). In the sediments there are outcrops of sulfide crusts and mounds with yellow patches indicating sulphur deposion (Fig. 21). Some of the sulfide deposits are shaped like pinnacles (Fig. 22).

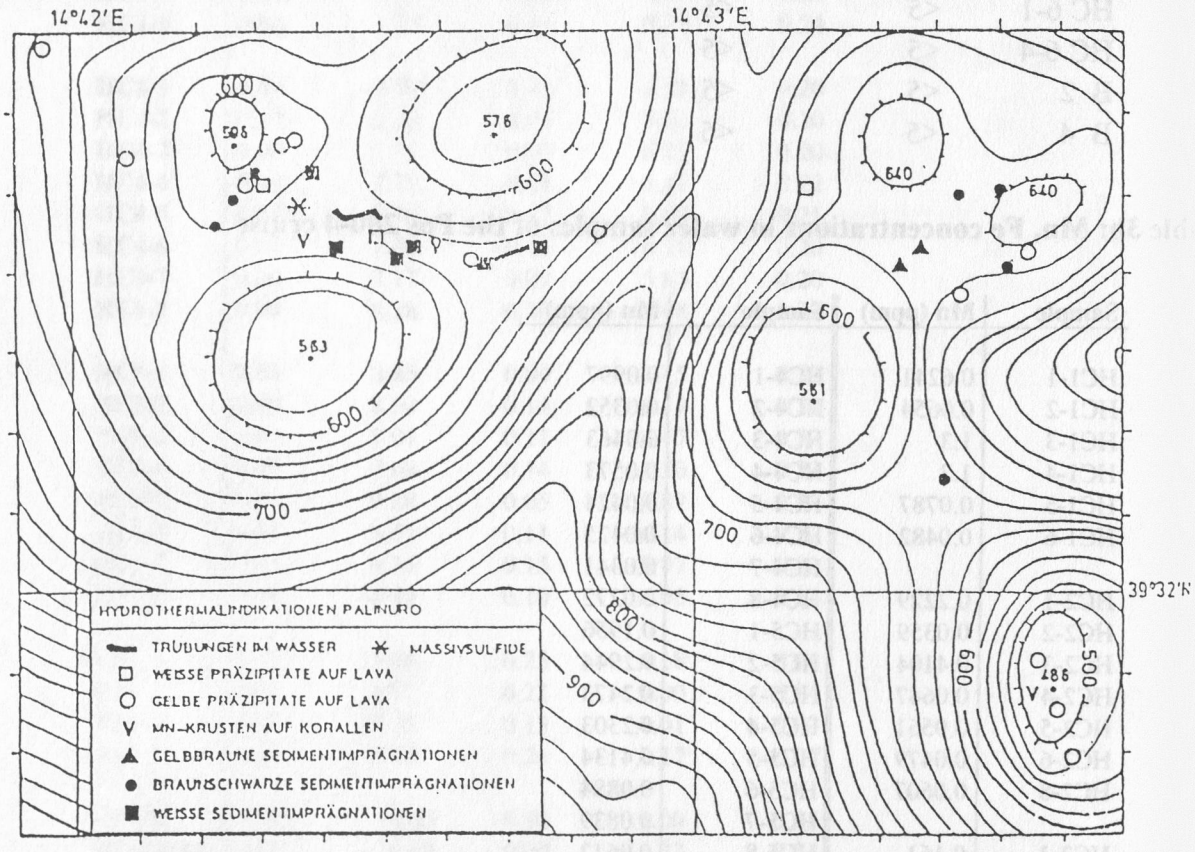

Abb.19: OFOS-Beobachtungen am Palinuro (FS 70) mit Probenahmepunkt der Massivsulfide (FG 181).

Some photos show carbonate crusts which are roughly layered. On these, and adjacent sediment there are yellow hydrothermal precipitates. White, biogenic traces on carbonate crusts slightly coated with Mn-oxide have been observed. Some photos show white precipitates (barite?) on dark crusts (fig. 23). Some white patches on dark sediment suggest the existence of bacterial activity.

In several places of the Palinuro E-peak the sediment exhibits heterogenous hydrothermal sediments, i.e. mottled, irregular patches of brown to light yellow, gray and white color. In some sites different hole types can be observed (Fig. 24). One type appears to consist of fresh, small holes and the other of altered collapsed holes. These are also sites with abundant, heterogenous crust fragments and with small Mn nodules (Minnitti and Bonavia, 1984).

In the Marsili investigation area, the lava appears to be scoria-rich and roughly sheeted (Savelli 1993). Near the site of sulfide outcrop at 39°17.11N and 14°23.86E at depth of 510 m, there are thin gray sediments. Isolated dark patches may consist of either Mn micronodules or volcanic ashes.

There are sites of 50 square m (Uchupi and Ballard, 1989) entirely covered by sulfide mounds and crusts. The mounds have thin Mn coating and are capped by yellow precipitates. The surrounding sediments has dark brownish to yellow precipitates. A picture shows a small colony of yellow tube-worms growing on lava talus. From the central part of the Palinuro area, which had been investigated by OFOS, four sediment cores had been taken (Stat. 358, 368, 357; Fig. 19). An overview of the sediment below profile description is given. All of the sediments are either influenced by hydrothermal solutions forming Fe-oxihydroxides (Stat. 357, 4-6cm, 28-42,5cm; Stat. 368 34-38cm; Stat. 358 ~ 20cm) or nontronites, or by volcanism forming ash layers (Stat. 357-1, 12-27cm; Stat. 357, 28-42,5cm).

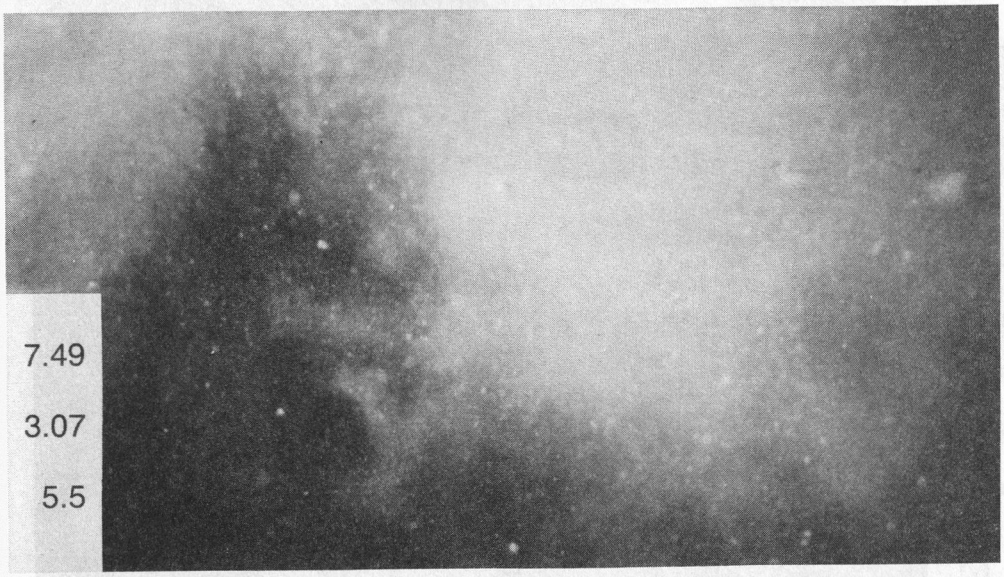

Figure 20: Turbid water at Palinuro Seamount

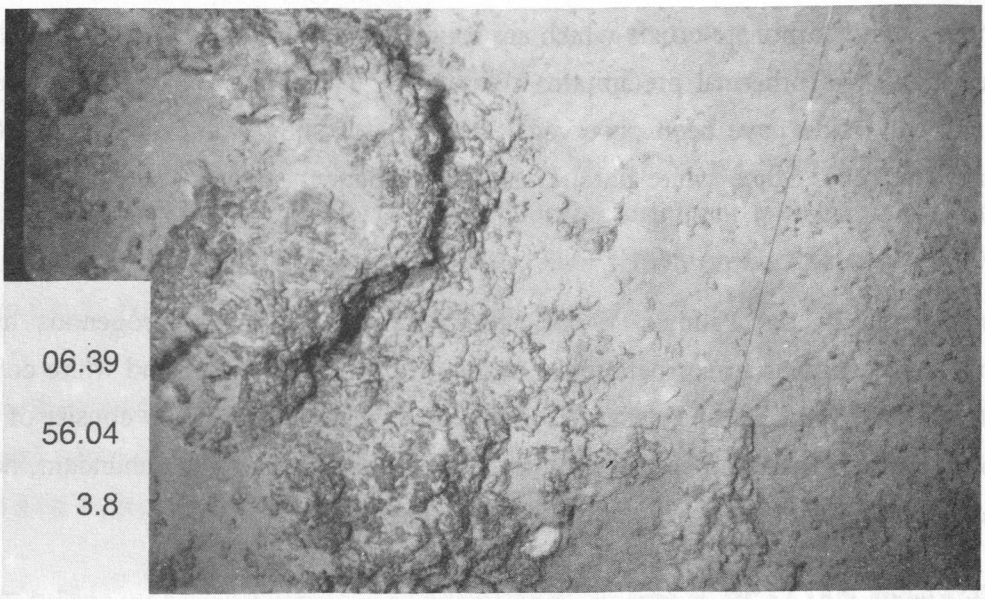

Figure 21: Sulfur Crust on Palinuro Seamount

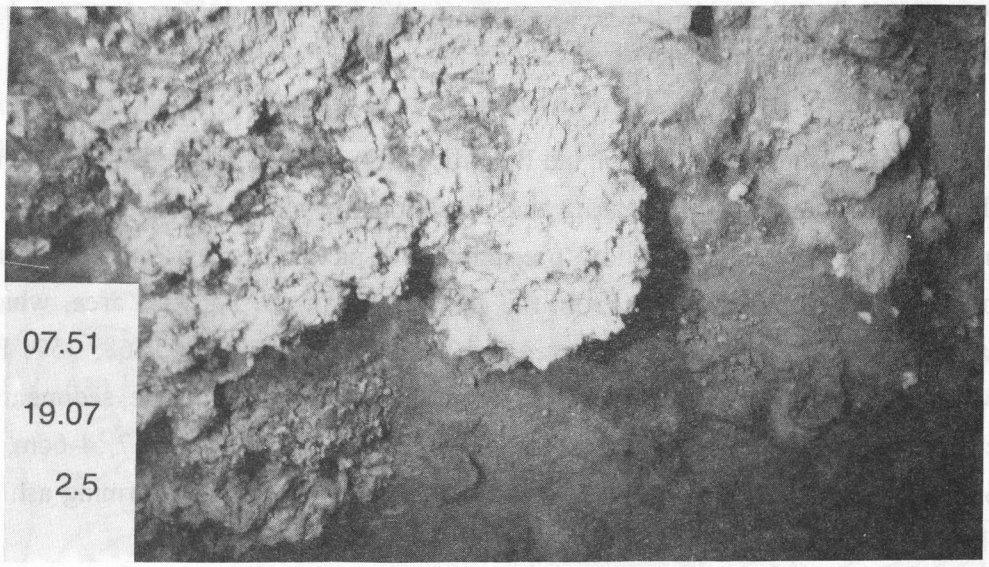

Figure 22: Sulfur pinnacles on Palinuro Seamount

Figure 23: Holes of biogenic origin covering the sediment

Sediment core description

Stat. 357
core length: 2.6cm
2 distinct layers:

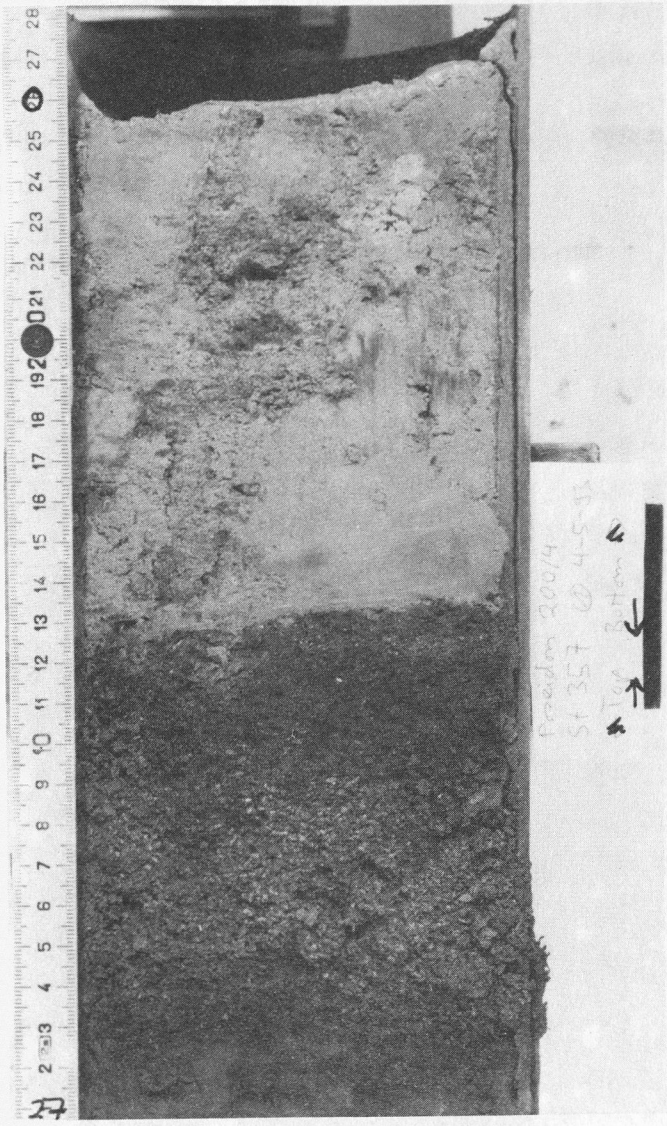

0-12.5cm
silty clay, greenish-grey
dark grey schlieres
small cavities

12.5-27
Ashlayer, greyish block
to dark grey (2N2-3N3)
sandy to coarse grain,
consolidates particles
of several cm thickness

Stat. 357
core length: 42.5cm
3 distinct layers

0-6cm
soft clay red-brown (5YR 6/4)
4-6cm more reddish, inclusion of a Fe-hydroxid fragment, 10cm thick as well as a Fe-hydroxid layer of 1cm tihckness.

6-28cm
soft clay patches of light grey, very light grey to moderate grey and yellowish-orange material, not layered

28-42.5cm
silty to sandy material dark grey (5YR 2/1)
ash material

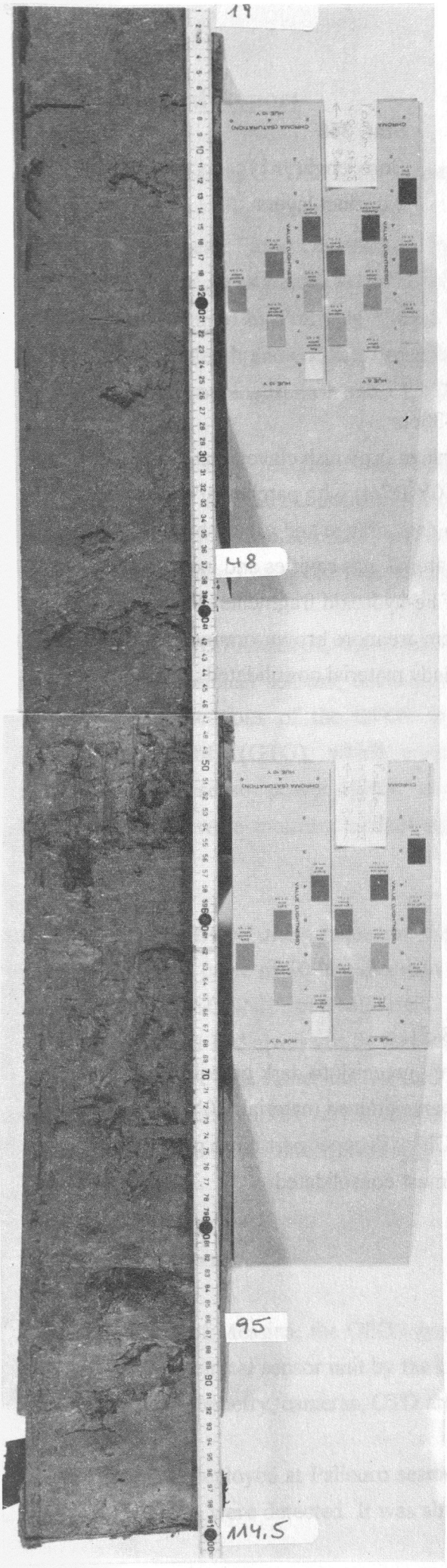

Stat 358
core length 114.5cm
distinct layers

0-10cm
soft clay,
light brown to moderate yellowish-brown (5YR 5/6, 10YR 5/4)

10-48cm
greenish-grey soft clay,
patches and schlieres of dark yellowish-orange clayey material
gas cavities of several cm size

48-95cm medium grey (5B/ 5/1)
clay material, soft gas cavities and schliering of light brownish-grey material inclusion of a 3cm thick rock material

95-114.5
light greenish-grey soft clay material (5G 8/1)

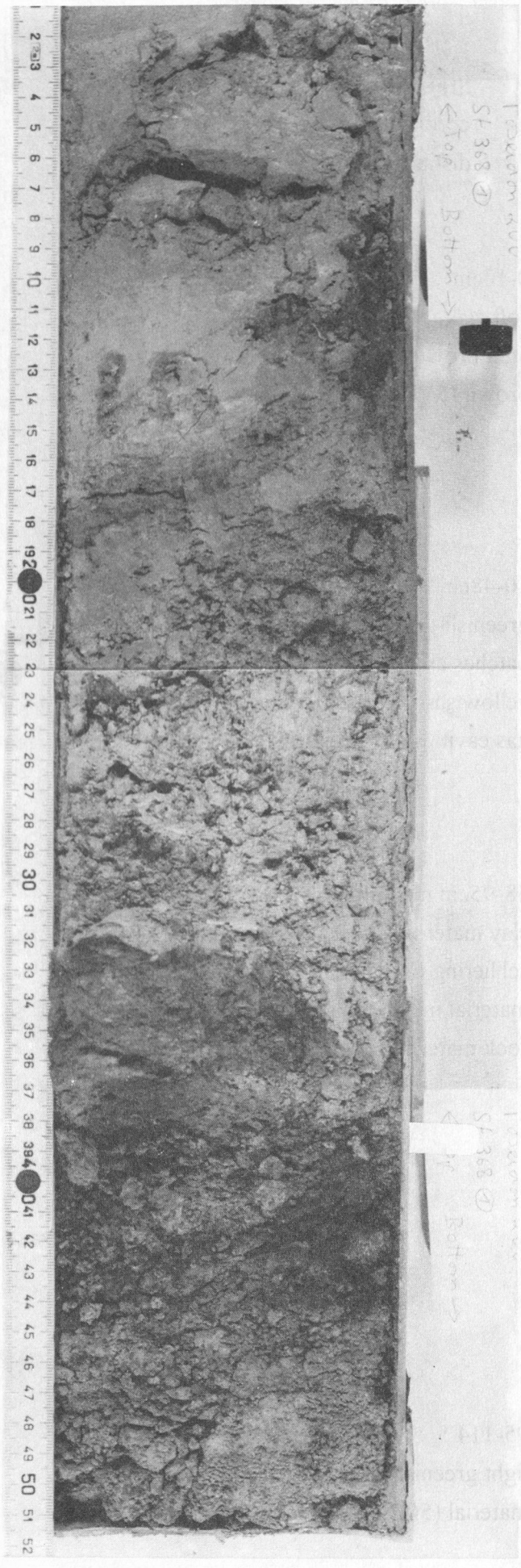

Stat. 368
Core lenght:h 51c
2 distinct layers

0-38cm
orange-brownish clayey material (10Y R7/4) with patches of dark brown to dark orange and greenish silty material, gas cavities and inclusion of Fe-hydroxid fragments. The upper 5cm are more brown-orange (5YR 5/6) silty to sandy material consilidated.

38-51cm
grey-greenish to dark greenish dry coarse grained material (10Y 6/2 to 5GY 4/1) upper part more grey-green almost consolidated

5. Technical Report

5.1 Survey System OFOS (GTG Group)

The so-called Ocean Floor Observation System OFOS, which was formerly known mainly as "TV/Photo sledge", was purchased by the Geological Institute of Kiel University (GIK) in 1988, and was manufactured by Preussag Marine Technology. This system is rated for operation down to 6000 m water depth and consists basically of a real-time video camera with flood lights, a high capacity photo camera with flash and a CTD probe.

Power supply (mainly for the flood lights) is achieved by pressure compensated lead-acid accumulators. TV and data transmission over one single coaxial cable is handled by the specially designed telemetry electronics. The system is connected to the ship via a steel-armoured coaxial cable, and is towed at low speed with bottom distances usually between 2 and 8 meters.

As a subject of MIPAMEHR, the OFOS is upgraded towards a multi-sensor survey tool by adding electro-chemical sensors, developed by the University of Newcastle upon Tyne (UNT). Necessary modifications of the OFOS for sensor integration had been done by GEOMAR Technologie GmbH (GTG), which comprized mechanical adaptions as well as electronic modifications for sensor power supply, sensor data interface and OFOS telemetry extension. For this cruise there were mounted additionally two Niskin water samplers with on-board release control.

On R/V "POSEIDON" the equipment was handled by an on-board winch with about 1800 m armoured coaxial cable of 10 mm diameter. This cable is rather thin compared to e.g. the 18 mm cables on R/V "SONNE" or "METEOR", so there is only little safety margin in mechanical strength. This fact had always to be taken into account during deployments, although fortunately on the cruise there was rather fair weather with low sea swell. As an other risk-reducing factor, the winch operators worked very accurate and always followed precisely the commands given to them from the laboratory through the ship's wire-com.

5.1.2. OFOS Operations

Still in the port of Messina, the OFOS system was made ready for set-up and tests of the latest version of the chemical sensor unit by the UNT group. After some adjustments the on-board tests showed OFOS telemetry, cameras, CTD and the sensor communication link in working order.

OFOS was first deployed at Palinuro seamount (Station 339). The main functions were working, but two problems were detected. It was already known from earlier cruises that from time to time

there occur short blackouts of the telemetry. There had been made investigations already by GTG, but even the original manufacturer could not find a solution. Usually this effect can be tolerated as it causes only short surges in the data stream and on the TV screen, but this time it was recognized that a black-out also can cause a water sampler to be closed.

So during nearly all the deployments one water sampler was closed by accident and not by manual control, only the other sampler still remained ready as its release was less sensitive. But sometimes it was even too unsensitive to be released by intention, although the electronics worked correctly.

The other problem concerned the CTD probe: as soon as the equipment was in the water, CTD data was distorted. This effect had been detected before but could never be reproduced in the workshop. Modifications made to the OFOS electronics prior to the cruise obviously had no effect. Only after the last deployment was it finally found out that the fault was in the probe itself. Once the failure was known it could be repaired on-board by P. Haushahn - unfortunately too late to be of benefit for this cruise.

But besides the described problems the system was operational during all the deployments. Video / photo cameras and the sensor data link worked continously during the 8 deployments between 60 and appr. 900 m water depth. One dramatic event occured during station 354 when the OFOS was stuck to a steep rock wall in 850 m depth. But by help of the efficient action of the ship's navigator the equipment could be freed after 10 minutes. Inspection on deck after recovery only showed minor damages to the frame and fortunately no damage to the tow cable. So the deployment could be continued with station 355 after short time.

5.1.3. Surface Navigation

To log the actual course of the ship during stations or profiles, a separate GPS satellite navigation receiver had been carried on R/V "POSEIDON". There exist two GPS systems already on board of the vessel, but the first is used exclusively for ship's navigation and no access for scientists is allowed for any understandable reasons. The second on-board GPS is an older Magnavox one which still performs very well and is available for scientists. But it is located on the bridge, and the digital interface provided there is an older parallel binary version which is not very common today.

So it was more feasible to have a third GPS receiver within the laboratory with a standard serial interface to an IBM compatible PC. By means of a special software, developed by the Institute of Applied Physics in Kiel, the position data was presented on a monitor screen and stored to hard disk for later use.

Unfortunately, this standard GPS device was also not without problems. The reason for this was the position of the antenna. Although mounted on the wheelhouse top, parts of the ship's mast could nonetheless shade some receiving directions. Thus, depending on satellite constellation and the ship's heading, from time to time the laboratory GPS could not receive the minimum of 3 satellites required for navigation.

5.1.4. Transponder Navigation

As the underwater position of a towed system like the OFOS may be different from the ship's position, varying with towing depth and speed, cable length, currents etc., an underwater navigation system is supplied for precise location of the towed vehicle. Those systems, working with acoustic methods, are commercially available.

Such a so-called transponder navigation system (Fig. 25) had been acquired by GTG from manufacturer MORS/OCEANO, France. Transponder navigation is based on the calculation of distances in water from run-time measurements of sound. The GTG Long Baseline System (see figure) consists of

- At least 3 acoustic transponders moored to the bottom
- A hydrophone towed near the surface (or fix mounted on ship)
- The underwater object with an additional transponder to be tracked
- An on-board computer with software for position calculation

The bottom transponders, rated for 6000 m water depth, are equipped with a floatation pack for recovery and can be released from the anchor weight by acoustic command. Navigation accuracy of the system is rated down to 1 m in repeatability under best conditions. System performance very much depends on quality of installation / calibration and sound propagation conditions.

First experiences had been made in 1992, showing that this type of systems is rather complex and in consequence is not to be operated very simple. On this cruise in the area of Palinuro seamount five bottom transponders had been deployed in Station 341 . As the morphology is not very smooth there, precise acoustic navigation could not be expected in some locations, where the signals of transponders were acoustically shaded by seamounts.

Before real navigation can start, a calibration process is needed with collection of data when

Fig. 25

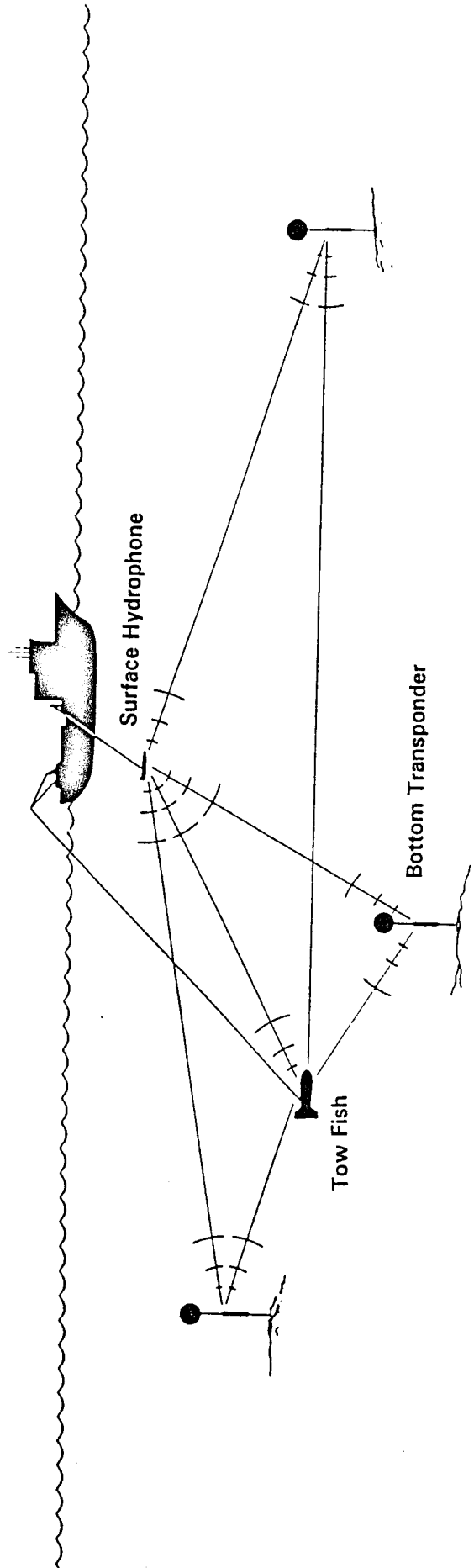

Long Baseline Transponder Navigation

steaming through the deployed array. Quality of this data acquisition, together with proper layout of array geometry, influences very much the actual system accuracy. To improve range calculations, a sound velocity profile derived from CTD data of water sampling stations was input to the navigation computer. The calibration data acquisition had been done at night after Station 341, there it was detected that one of the transponders was not responding, thus leaving only 4 bottom references.

During OFOS stations 354 and 355 the transponder navigation was operated, but only tracking of the surface hydrophone, i.e. the ship's position, worked properly. As soon as underwater tracking was selected, the software crashed. It should be noted though, that even surface navigation only, but with reference to the bottom transponders, is of higher quality than a GPS navigation. The latter only is reliable within a magnitude of 100-200 m, a properly calibrated long baseline navigation within some meters.

As a result of contacts with MORS/Oceano and several hours spent before the computer during the following days, some configuration data was modified. So during OFOS station 367 also underwater tracking was in use. The results however were rather poor, as the calculated underwater position frequently was unsteady and thus not reliable. One reasons possible might be the critical acoustic situation. Navigation data logged on this cruise will be discussed later with MORS/Oceano to determine on explanation.

No more stations were carried out with transponder navigation, during station 368 and the bottom transponders were recovered. All of them could be released by acoustic command without problems, even the one which had not been responding for navigation. Thanks to the excellent navigation of the ship, within short time all five transponders were collected.

5.2. Exploration with the sensor package of the OFOS system

In order to better understand the effect of submarine hydrothermal activity on water columns and to facilitate the real-time mapping of hydrothermal plumes so as to locate sites of active seafloor vents and associated mineral deposits a chemical sensor package was included into the OFOS system.

Before the deployment of the system at the summit of Palinuro Seamount the sensor system was mechanically and electronically checked and calibrated for quantitative analysis. On inspection it was realised that case 2 electronics of ASCREV 2 were badly corroded and it was decided not to deploy ASCREV 2, that means that we could either measure Mn or Fe content.

The system was set up for calibration with preplating and ligand ring set up for one ASCREV cell only - Fe. The calibration was started as per handbook flowing seawater, temperature 17C°,

flowrate 45ml/min for the particular calibration routine used pH 4, 7, 9; Fe, O_2, S^{2-}: 0.01, 0.1, 1.0 mmol; Eh; H_2S, calibration of the H_2 sensor was not attempted as there appeared to be a fault with the output remaining unchanged and too constant suggesting an electrical problem or an insensitive sensor. Time taken for calibration was too long, therefore the calibration procedure has been modified.

After the first deployment it was found out that:

- case 2 had been leaking (about half full of water),
- case 3 had been some leakage/ weeping from the lower end of the pH unit,
- the end plate on the electronics was twisting (brass support rods had sheared),
- the buffer board which was mounted near the passives was soaked,
- the pH electrode was damaged,
- the PTFE body of the O_2 sensor had been deformed,
- there was bery fine silt on the passive and gas sensors,
- cracking was noticed where the metal fitting entered the filter housing unit.

A repair programme and another check was started. ASCREV 1 was set up for Mn determinations and a calibration run was undertaken but stopped shortly because of electronic problems. Because of big delay it was decided to make a second deployment and the calibration afterwards.

After the 2nd deployment it was found out that:

- case 2 had liquid in it,
- case 3 had a leakage,
- the reference readings were uncorrect and the socket was not in correctly, the plastic guide which would only allow the socket to go in the one way was broken off.

While starting the calibration run, it was found out that the pump was not operational. The pump casing was opened and it was found out that the leads had come away from the internal plug at the pins - they appeared to have just broken off or corroded. The second pump was installed. A small hole in the plastic pipe between the pump and the filter was recognized producing air bubbles. Further problems were:

- no flow through case 3 because of current cut out from the power supply caused by the pump,
- corrosion on the four way connector.

The next step was to put the two pumps into the pump housing, however the pipe work was fouling on the edges of the pump and would not go into the tube. It was decided just to put the refurbished pump in on its own. After powering up the system again the temperature information from case 3 was suspect due to some spiking on the temperature transducer, which was exchanged.

For the deployment a new temperature transducer was plumbed in, gas sensors were checked to be potentiostating. The buffer board was put into a plastic bag which was taped, and then all the casings were sealed and the OFOS deployed.

After the third deployment, a calibration run was going to start. However, further problems with the pump motor occured. The pump was again repaired using the motor contacts from the other pumps.

The system was set up again for another deployment. However, the data were overloaded as a result of an impressed potential, probably from the reference electrode buffer board. The system was deployed (4th deployment) in order to complete the OFOS profile (video and camera run) of Palinuro Seamount, however, power to the pump was disconnected. After the run the electronics were completely checked. Besides this it was found out that case 3 had again a leakage. Problems appeared, such as:

- buffer board with the gas sensors showed interference effect to the buffer amplifier associated with the passive reference electrode,
- gas sensors were not working.

The gas sensors as well as the pump were repaired and checked. The buffer board was now fully functional as well as the 3 electronic parts of the 3 sensors (passive, gas and temperature). Whilst the system was set up again it was found out that due to corrosion a lot of wires became very brittle and disconnected. They were replaced and it was decided to deploy the system again with case 3 connected but ASCREV 1 disconnected because there was no flow-through of both cases.

After the 5th deployment a calibration run was attempted for pH, Eh, S^{2-} and O_2. The gas sensors were overloaded. It was noticed that there was a blockage in case 3 - grit was found in the H_2S sensor. The calibration run was stopped. During the check it was found out that:

- the menbranes of the gas sensors were damaged, caused probably by pressure effects,
- again grit-like material (~ 2-3mm in size) appeared in the H_2S sensor,
- electronics of case 3 caused problems,
- leakage occurred in case 3, water had dripped into the plastic bag containing the buffer board. The buffer board was now unusuable.

During the Poseidon 200-4 cruise it was not possible to use the sensor system of the OFOS on a scientific base as a lot of problems occurred due to leakages, brake downs, pressure compensation effects etc.

6. References

AGIP (1981) Carta magnetica d'Italia: Anomalie del campo magnetico redisuo. 1/500,000, sheet M.

Allert, P. (1978) Thesis, Univ. Paris.

Arisi Rota, F. and Fichera, R. (1987) Magnetic interpretation related to geo-magnetic provinces: the Italian case history. Tectonophysics, 138: 179-196.

Atzori, P., Ghisetti, F., Pettino, A. and Vezzani, L. (1978) Strutture et evoluzione geodinamica recente dell'area peloritana (Sicilia nor-orientale). Boll. Soc. Geol. Ital., 97: 31-56.

Badalamenti, B., Falsaperla, S., Neri, G., Nuccio, P.M. and Valenza, M. (1986) Confronto preliminare tra dati sismici et geochimic nell'area Lipari-Vulcano. Boll. GNV, 2: 37-47.

Barberi, F., Innocneti, F., Ferrara, G., Keller, J. and Villari, L. (1974) Evolution of Aeolian arc volcanism (Southern Tyhhrenian Sea). Earth Planet. Sci. Lett., 21: 269-276.

Beccaluva, L., Bonatti, E., Dupuy, C., Ferrara, G., Innocenti, F., Lucchini, F., Macera, P., Petrini, R., Rossi, P.L., Serri, G., Seyler, M. and Siena, F. (1990) Geochemistry and mineralogy of volcanic rocks from ODP sites 650, 651, 655 and 654 in the Tyrrhenian Sea. Proceedings of the Ocean Drilling Program, Scientific Results, Vol. 107: 49-74.

Beccaluva, L., Gabbianelli, G., Lucchini, F., Rossi, P.L. and Savelli, C. (1985) Petrology and K/Ar ages of volcanics dredged from the Aeolian seamounts; implications for geodynamic evolution of the southern Tyrrhenian basin. E.P.S.L. 74: 187-208.

Beccaluva, L., Gabbianelli, G., Lucchini, F., Rossi, P.L., Savelli, C. and Zeda, O. (1981) Magamtic character and K/Ar ages of volcanics dredged from the Aeolian seamounts (Tyrrhenian Sea). IN: F.C. Wezel (ed.), Sedimentary Basins of Mediterranean Margins. Tecnoprint, Bologna, pp. 361-368.

Belderson, H.B., Kenyon, N.H. and Stride, A.H. (1974) Features of submarine volcanoes shown on long range sonographs. J. Geol. Soc. London, 130: 403-410.

Bertrand, H., Boivin, P. and Robin, C. (1990) Petrology and geochemistry of basalts from the Vavilov Basin (Tyrrhenian sea), Ocean drilling program Leg 107, Holes 651A and 655B. Ocean Drilling Program, Scientific Results, Vol. 107: 49-74.

Boccaletti, M., Nicolich, R. and Tororici, L. (1984) The Calabrian Arc and the Ionian Sea in the dynamic evolution of the Central mediterranean. Mar. Geol., 55: 219-245.

Bocchi, G., Lucchini, F. and Rossi, P.L. (1979) Dati mineralogici e geochimici su un deposito manganesifero sottomarino del Mar tirreno. Mineral. Petrogr. Acta, 23: 99-109.

Bonasia, V., Nappi, G. and Pingue, F. (1985) Ground deformation, volcanism and neotectonics at Lipari and Vulcano Islands (Southern Tyrrhenian Sea). Ann. Geophysicae, 3: 793-798.

Budetta, G., Nunziata, C. and Rapolla, A. (1983) A gravity study of the island of Vulcano, Tyrrhenian Sea, Italy. Bull. Volcanol., 46: 183-192.

Calanchi, N., Luchhini, F., Rossi, P.L. and Bocchi, G. (in press) Structural evolution and magmatic character of the volcanic complex of Panarea (Aeolian Islands, Italy). Tectonophysics.

Carapezza, M., Nuccio, P.M. and Valenza, M. (1981) Bull. volcan., 44: 547-563.

Carapezza, M., Nuccio, P.M. and Valenza, M. (1986) Extensive and intensive parametersin the geochemical surveillance of volcanic activity: some examples in Italy. Internat. Volcanol. Comgress, New Zealand.

Carbone, S., Grasso, M. and Lentini, F. (1982) Considerazioni sull'evoluzione geodinamica della Sicilia sudorientale dal Cretaceo al Quaternario. Mem. Soc. Geol. Ital., 24: 367-386.

Ciabatti, M. (1970) Sedimenti dei monti sottomarini. In: Selli (ed.), Ricerche geologiche preliminari nel Mar Tirreno. G. Geol., 37: 73-88.

Cioni , R. and D'Amore, F. (1984) A genetic model for the crater fumaroles of Vulcano Island (Sicily, Italy). Geothermics, 13: 375-384.

CNR-GNV (1988) Intervento straordinario a Vulcano. Estate 1988, Roma.

Cochran, J. (1981) The gulf of Aden: Structure and evolution of a young ocean basin and continental margin. J. Geophys. Res., 86 (B1): 263-287.

Colantoni, P., Lucchini, F., Rossi, P.L., Sartori, R. and Savelli, C. (1981) The Palinuro volcano and magmatism of the SE Tyrrhenian sea (Mediterranean). Marine Geol., 39: 1-12.

Cortese, M., Frazzetta, G. and La Volpe, L. (1986) Volcanic history of Lipari (Aeolian Islands, Italy) during the last 10,000 years. J. Volcanol. Geotherm. Res., 27: 117-133.

Del Monte, M. (1972) Il vulcanesimo del Mar Tirreno: nota preliminare sui vulcani Marsili e Palinuro. G. Geol., 38: 231-252.

Di Girolamo, P. (1978) Geotectonic settings of Miocene-Quaternary vulcanism in and around the Eastern Tyrrhenian sea border (Italy) as deduced from the major elements geochemistry. Bull. Volcanol., 41: 229-250.

Doglioni, C. (1991) A proposal of kinematic modeling for W-dipping subduction - Possible applications to the Tyrrhenian-Apennines system. Terra Nova, 3: 423-434.

Edmond, J.M., Measures, C., McDuff, R.E., Chan, L.H., Collier, R., Grant, B., Gordon, L.I. and Corliss, J.B. (1979) Ridge crest hydrothermal activity and the balances of the major and minor elements in the ocean.. The Galapagos data. Earth Planet Sci Lett 46: 1-18.

Eriksson, L. and Savelli, C. (1989) Magnetic anomalies and magmatic events in and around the island of Elba (Northern Tyrrhenian Sea). Marine Geol., 87: 85-93.

Fabbri, A., Marabini, F. and Rossi, S. (1973) Lineamenti geomorfologici del Monte Palinuro e del Monte delle Baronie (Mar Tirreno). G. Geol., 39: 133-156.

Falsaperla , S. and Neri, G. (1986) Contributi sismologici alla sorveglianza vulcanica di Vulcano. Boll. GNV, 2: 243-254.

Feraud, G. (1990) 39Ar-40Ar analysis of basaltic lava series of Vavilov basin, Tyrrhenian Sea. (Ocean drilling program, Leg 107, Holes 655B and 651A). Proceedings of the Ocean Drilling Program, Scientific Results, Vol. 107: 93-97.

Ferri, M., Grimaldi, M. and Luongo, G. (1988) Vertical ground deformation on Vulcano, Aeolian Islands, Southern Italy: observations and interpretations 1976-1986. J. Volcanol. Geotherm. Res., 35: 141-150.

Ferrruci et al., (1989) Geophys. Res. Lett., 16: 1317-1320.

Finetti, I. and Del Ben, A. (1986) Geophysical study of the Tyrrhenian opening. Bull. Geof. Teor. Appl., 28 (110): 75-155.

Frazetta, G., Gillot, P.Y., La Volpe, L and Sheridan, M.F. (1984) Volcanic hazards at Fossa of Vulcano: data from the last 6,000 years. Bull. Volcanol., 47: 105-124.

Frazetta, G., Lanzafame, G. and Villari, L. (1982) Deformazioni e tettonica attiva a Lipari e Vulcano (Eolie). Mem. Soc. Geol. It., 24: 294-297.

Frazzetta, G. and La Volpe, L. (1987) Storia eruttiva dell'isola di Vulcano: stato di avanzamento della ricerca. Boll. GNV, 3: 361-372.

Frazzetta, G., La Volpe, L. and Sheridan, M.F. (1983) Evolution of the Fossa cone, Vulcano. J. Volcanol. Geotherm. Res., 17: 329-360.

Gabbianelli, G., Curzi, P. and Selli, L. (1983) The Stromboli canyon (Tyrrhenian Sea). Abstracts 4th I.A.S. European Meeting, 59-61.

Gabbianelli, G., Gillot, P.Y., Lanzafame, G., Romagnoli, C. and Rossi, P.L. (1990) Tectonic and Volcanic Evolution of Panarea (Aeolian Islands, Italy). Marine Geology, 92: 313-326.

Gabbianelli, G., Romagnoli, C., Rossi, P.L., Calanchi, N and Lucchini, F. (1991) Submarine morphology and tectonics of Vulcano (Aeolian Islands, Southeastern Tyrrhenian Sea). Acta Vulcanologica, 1: 135-141.

Ghisetti, F. and Vezzani, L. (1981) Conribution of structural analysis to understanding the geodynamic evolution of the Calabrian arc (Southern Italy). J. Struct. Geol., 3: 371-381.

Got, H., Mirabile, L., Monaco, A. and Valette, J.N. (1978) Structure du recuvrement sedimentaire entre les Iles Eoliennes et la Sicile. Rev. Geogr. Phys. Geol. Dynam., 20: 415-422.

Hooker, Bertami, R., Lombardi, S., O'Nions, R.K. and Oxburgh, E.R. (1985) Geochim. Cosmochim. Acta, 49: 2505-2531.

HYMAS I, 1986. Forschungsfahrt Sonne 41, Fahrtbericht, Projektleitung von H. Puchelt, erstellt von D. Laschek, Univ. Karlsruhe, pp. 331 (pre-print).

Kastens, K., Mascle, J., Auroux, C. and Coll., ODP Leg 107 Scientific Party (1988). ODP Leg 107 in the Tyrrhenian sea: Insights into passive margin and back-arc basin evolution. Geol. Soc. Amer. Bull., 100: 1140-1156.

Keller , J. (1980) The Island of Vulcano. Rend. Soc. It. Miner. Petrol., 36: 489-534.

Kidd, R.B. and Armansson, H. (1979) Manganese and iron micronodules from a volcanic seamount in the Tyrrhenian sea. J. Geol. London, 136: 7176.

Lanzafame, G. and Rossi, P.L. (1984) Evidneze di attivita'tettonica recente a Panarea (Eolie): implicazioni vulcanologiche. Geol. Rom., 23: 131-139.

Lavecchia, G. (1988) The Tyrrhenian-Apennines system: structural setting and seismottectogenesis. Tectonophys., 147: 263-296.

Lavecchia, G. and Stoppa, F. (1990) The Tyrrhenian zone: a case of lithosphere extension control of intra-continental magamtism. Earth Planet. Sci. Lett., 99: 336-350.

Lo Giudice, E., Marino, C.M. and Tonelli, A.M. (1975) Le tecniche di ripresa all'infrarosso termico applicate ai rielievi aerei dell'isola di Vulcano. Analisi dei resultati in rapporto alla situazione geovulcanologica locale. Boll. Geof. Teor. Appl., 17: 19-38.

Locardi, E. and Nicolich, R. (1992) Geodinamica del Tirreno e dell' Appennino centro-meridionale: la nuova carta della Moho. Mem. Soc. Geol. It., 41 (1988): 121-140.

Martini , M. (1986) Sorveglianza geochimica del vulcanesimo attivo. Boll. GNV, 2: 337-346.

Martini, M., Cellini Legittimo, C., Piccardi, G. and Giannini, L. (1986) Geothermics, 15: 205-209.

Mazor et al., (1988) Bull. Volcan., 50: 71-85.

Minniti and Bonavia (1984) Marine Geol., V. 59, p. 271-282.

Minniti, M. and Boanvia, F. (1984) Copper-ore grade hydrothermal mineralization discovered in a seamount in the Tyrrhenian Sea (Mediterranean): is the mineralization related to porphyry-coppers or to base metal lodes? Marine Geol, 59: 271-282.

Morten, L., Landini, F., Bocchi, G., Mottana, A. and Brunfelt, A.O. (1980) Mn-Fe crusts from the south Tyrrhenian sea. Chem. Geol., 28: 261-278.

Mottl, M.J. (1983) Metabasalts, axial hot springs, and the structure of hydrothermal systems at mid-ocean ridges. Geol. Soc. Geol., 28: 261-278.

Moussat, E., Rehault, J.P. and Fabbri, A. (1986) Rifting et évolution tectonosédimentaire du Bassin Tyrrhénien au cors du Néogène et du Quarternaire. G.Geol., 48/1-2 (3): 41-62.

Polyak, B.G. et al., (1979) Dokl. Akad. Nauk. USSR, 247: 1120-1125 (in Russian).

Puchelt, H. and Laschek, D. (1986) Fahrtbericht SONNE 41, Inst. f. Petrog. und Geochem., Univ. Karlsruhe.

Rabbi , E. (1970) Ricerche chimiche e geochimiche. In: Selli (ed.), Ricerche geologiche preliminari nel Mar Tirreno. G. Geol., 37: 109-128.

Rehault, J.P., Mascle, J., Moussat, E. Fabbri, A. and Thommeret, M. (1987) The Thyrrenian sea before Leg 107. Proceedings of the Ocean Drilling Program, Initial Reports (Part A), Vol. 107: 9-35.

Rehault, J.P., Moussat, E. and Fabbri, A., 1987: Structural evolution of the Tyrrhenian back-arc basin. Marine Geology, 74: 123-150.

Rossi, P.L., Bocchi, G. and Lucchini, F. (1980) A manganese deposit from the south Tyrrhenian region. Oceanol. Acta, 3: 109-128.

Sano, Y., Wakita, H., Italiano, F. and Nuccio, M. (1979) Geophys. Rs. Lett., 16: 511-514.

Savelli , C. (1988) Late Oligocene to Recent episodes of magamtism in and around the orogenic (Mediterranean) type. In: F.C. Wezel (ed.), The origin of arcs. Tectonophys., 146: 163-181.

Savelli , C. and Schreider, A.A. (1991) The opening processes in the deep Tyrrhenian basins of Marsili and Vavilov as deduced from magnetic and chronological evidence of their igneous crust. Tectonophys., 190: 119-131.

Savelli , D. and Wezel, C.F. (1979) Morfologia e stile tettonico del bacino Tirrenico. Atti Conv. Scient. P.F. Ocenaografia e Fondi Marini, CNR, Roma.

Savelli, C. (1993) Giorn. Geol., v. 52/2 (1992), p. 215-227.

Scandone, P. (1979) Structure and evolution of the Calabrian Arc. Earth. Evolut. Sci., 3: 172-180.

Sedwick, P.N., McMurtry, G.M. and Macdougall, J.D. (1992) Chemistry of hydrothermal solutions from Pele`s Vents, Loihi Seamount, Hawaii. Geochim. Cosmochim. Acta 56: 3643-3667.

Selli , R. (1970) Profili magnetometrici. In: Selli (ed.), Ricerche geologiche preliminari nel Mar Tirreno. G. Geol. 37: 43-53.

Selli, R. (1974) Appunti sulla geologia del Mar Tirreno, Rend. Sem. Fac. Sc. Univ. Cagliari, suppl. 327-349.

Selli, R. (1981) Thoughts on the geology of the Mediterranean region. In: F.C. Wezel (ed.), Sedimentary Basins of Mediterranean Margins. Tecnoprint, Bologna, pp. 489-501.

Selli, R. and Gabbianelli, G. (1979) I depositi ferromanganesiferi del SE Tirreno. Atti Convegno CNR, Oceanografia e Fondi marini.

Sicardi, L. (1941) Bull. Volcan., 7: 85-140.

Tedesco et al., (1988) Scientific Event Alert Network (SEAN) Bull., 13 (5): 10-11.

Uchupi, E. and Ballard, R.D. (1989) Deep-Sea Research, V. 36, p. 1443-1448.

Wezel , F.C. (1985) Structural features and basin tectonics of the Tyrrhenian Sea. In: Geological evolution of the Mediterranean basin (D.J. Stanley and F.C. Wezel eds). Springer Verlag, New York, 153-194.

7. Appendix

Appedix 1: Station Reports

STATION REPORTS - Research cruise Poseidon 200-4

Station No:	**335 SL**
Sampler type:	sediment corer
Area:	Marsilli Basin
Date:	01.05.93
Latitude:	38°59'64N
Longitude:	15°02'46E
Water depth:	2750m
Station time (UTC):	6:33-9:25
Total time (min):	172
Remarks:	wire 2852m touched bottom
Samples:	no sediment

STATION REPORT

Station No.:	**336 SL**
Sampler type:	sediment corer 6m
Area:	Masrsilli Basin
Date:	01.05.93
Latitude:	38°59'29N
Longitude:	15°02'02E
Water depth:	2760m
Station time (UTC):	9:46-11:23
Total time (min):	97
Remarks:	tensiometer and length of wire show discrepancies
Samples:	no sediment

STATION REPORT

Station No.:	**337 SL**
Sampler type:	sediment core, 6m
Area:	Marsilli Basin
Date:	01.05.93
Latitude:	39°07'09N
Longitude:	15°08'00E
Water depth:	2500m
Station time (UTC):	13:10-14:00
Total time (min):	50
Remarks:	length of wire seems to be wrong
Samples:	sediment core of 4.10m length solid, layered sediment, clayey grey-green layers interlain by mm or 10s of m thick sandy layers, showing glittering particles and mm thick biogenous fragments.

STATION REPORT

Station No.:	**338 SL**
Sampler type:	Sediment corer, 12m
Area:	Marsilli Basin
Date:	01.05.93
Latitude:	39°07'02N
Longitude:	15°09'04E
Water depth:	2510m
Station time (UTC):	14:55-15:34
Total time (min):	39
Remarks:	
Samples:	930cm long sediment core sediment dense, layered like 337 SL.

STATION REPORT

Station No.:	**339**
Sampler type:	Extended OFOS
Area:	Palinuro Smt
Date:	02.05.93
Latitude:	39°32'27N
Longitude:	14°42'16E
Water depth:	559m
Station time (UTC):	7:22-9:52
Total time (min):	150
Remarks:	Bo-Co (T=13,9°C; P=334dB; Cond=35.5ms)
Samples:	400 photos, 150 min of video

STATION REPORT

Station No.:	**340 MS**
Sampler type:	multiprobe + water rosette
Area:	Palinuro Smt
Date:	02.05.93
Latitude:	39°32'43N
Longitude:	14°42'39E
Water depth:	650m
Station time (UTC):	15:54
Total time (min):	20
Remarks:	
Samples:	HC1-1 - HC1-6 6x5l water samples 6x60ml for Cl determination 6x _40ml (frozen) samples for nutrient determination 6x1l filtered acidified samples

STATION REPORT

Station No.:	**341**
Sampler type:	5 transponder
Area:	Palinuro Smt
Date:	02.05.93
Latitude:	see transponder reports
Longitude:	
Water depth:	
Station time (UTC):	16:41
Total time (min):	100
Remarks:	successful
Samples:	

STATION REPORT

Station No.:	**342 BG**
Sampler type:	sediment grab
Area:	Palinuro Smt
Date:	03.05.93
Latitude:	39°32'29N
Longitude:	14°41'90E
Water depth:	614m
Station time (UTC):	6:00-6:46
Total time (min):	46
Remarks:	
Samples:	hydrothermal crust covered by brown soft muddy sediment; 1 top sample, 1 hydrothermal crust sample, 1 entire sample.

STATION REPORT

Station No.:	**343 BG**
Sampler type:	sediment grab
Area:	Palinuro Smt
Date:	03.05.93
Latitude:	39°32'38N
Longitude:	14°41'39E
Water depth:	630m
Station time (UTC):	7:00-7:30
Total time (min):	30
Remarks:	
Samples:	grey soft muddy sediment covered by brown soft muddy sediment; 1 top sample, 1 entire sample

---

STATION REPORT

Station No.:	**344 BG**
Sampler type:	sediment grab
Area:	Palinuro Smt
Date:	03.05.93
Latitude:	39°32'476N
Longitude:	14°42'372E
Water depth:	596m
Station time (UTC):	7:47-8:15
Total time (min):	27
Remarks:	
Samples:	no sediment

STATION REPORT

Station No.:	**345 BG**
Sampler type:	sediment grab
Area:	Palinuro Smt
Date:	03.05.93
Latitude:	39°32'482N
Longitude:	14°42'226E
Water depth:	579m
Station time (UTC):	8:17-8:45
Total time (min):	28
Remarks:	
Samples:	Piece of coral encrusted of Mn; Sediment comparable to that of St. 342 but just brown mud with pieces of hydroth. sediment; 1 entire sample

---

STATION REPORT

Station No.:	**346 MS**
Sampler type:	multiprobe + water rosette
Area:	Palinuro Smt
Date:	03.05.93
Latitude:	39°32'51N
Longitude:	14°42'26E
Water depth:	580m
Station time (UTC):	9:13-9:38
Total time (min):	25
Remarks:	
Samples:	HC2-1 - HC2-8 6x5l water samples 6x60ml for Cl determination 6x40ml samples for nutrient determination 6x1l filtered acidified samples

STATION REPORT

Station No.:	**347 BG**
Sampler type:	sediment grab
Area:	Palinuro Smt
Date:	03.05.93
Latitude:	39°32'00N
Longitude:	14°14.53E
Water depth:	590m
Station time (UTC):	9:51-10:07
Total time (min):	16
Remarks:	
Samples:	no sediment

STATION REPORT

Station No.:	**348 BG**
Sampler type:	sediment grab
Area:	Palinuro Smt
Date:	03.05.93
Latitude:	39°31'92N
Longitude:	14°43'44E
Water depth:	553m
Station time (UTC):	10:26-10:45
Total time (min):	19
Remarks:	grab did not close
Samples:	no sediment

STATION REPORT

Station No.:	**349 BG**
Sampler type:	sediment grab
Area:	Palinuro Smt
Date:	03.05.93
Latitude:	39°32'29N
Longitude:	14°43'23E
Water depth:	616
Station time (UTC):	11:00-11:20
Total time (min):	20
Remarks:	grab did not close
Samples:	no sediment

STATION REPORT

Station No.:	**350 BG**
Sampler type:	sediment grab
Area:	Palinuro Smt
Date:	03.05.93
Latitude:	39°31'32N
Longitude:	14°43'26E
Water depth:	618m
Station time (UTC):	12:01
Total time (min):	17
Remarks:	
Samples:	nodules of hydrothermal origin soft sediment with (2-3mm) black fragments

STATION REPORT

Station No.:	**351 DS**
Sampler type:	dredge
Area:	Palinuro Smt
Date:	03.05.93
Latitude:	39°42'43N
Longitude:	14°42'38E
Water depth:	639m
Station time (UTC):	12:20-13:36
Total time (min):	76
Remarks:	
Samples:	carbonat crust coated by Mn and Fe; compacted nontronite hydrothermal solid Fe-sediments; Fe-hydroxid layers; fragments of nontronite, covered with Mn; coral fragments, covered with Mn

---

STATION REPORT

Station No.:	**352 DS**
Sampler type:	dredge
Area:	Palinuro Smt
Date:	03.05.93
Latitude:	39°31'54N
Longitude:	14°39'82E
Water depth:	868m
Station time (UTC):	14:28-15:47
Total time (min):	79
Remarks:	
Samples:	Brown mud (thicker than in St. 351) over green mud, Mn crusts enclose, Fe-sediments, Fe-hydroxide, and nontronite in particular: veins of fresh Mn in compact brown mud (steriodal form)

STATION REPORT

Station No.:	**353 MS**
Sampler type:	multiprobe + water rosette
Area:	Palinuro Smt
Date:	03.05.93
Latitude:	39°32'39N
Longitude:	14°42'37E
Water depth:	650m
Station time (UTC):	17:15
Total time (min):	20
Remarks:	
Samples:	HC3-1 - HC3-8 8x5l water samples 8x60ml for Cl determination 8x40ml samples for nutrient determination 1l filtered acidified samples

STATION REPORT

Station No.:	**354 OFOS**
Sampler type:	Extended OFOS
Area:	Palinuro Smt
Date:	04.05.93
Latitude:	39°32'48N
Longitude:	14°42'16E
Water depth:	712m
Station time (UTC):	6:52-11:25
Total time (min):	273
Remarks:	
Samples:	420 photos, 270 min of video 354-1 1x5l water samples 60ml for Cl determination _ 40ml samples for nutrient determination 1l filtered acidified samples

STATION REPORT

Station No.:	**355 OFOS**
Sampler type:	Extended OFOS
Area:	Palinuro Smt
Date:	04.05.93
Latitude:	39°31'33N
Longitude:	14°39'64E
Water depth:	667m
Station time (UTC):	12:30-14:50
Total time (min):	140
Remarks:	
Samples:	134 photos, 140 min of video 355-1 1x5l water samples 60ml for Cl determination _ 40ml samples for nutrient determination 1l filtered acidified samples

STATION REPORT

Station No.:	**356 MS**
Sampler type:	multiprobe + water rosette
Area:	Palinuro Smt
Date:	04.05.93
Latitude:	39°31'30N
Longitude:	14°39'50E
Water depth:	150m
Station time (UTC):	15:40-16:13
Total time (min):	33
Remarks:	
Samples:	HC4-1 - HC4-8 8x1l water samples (1l for O_2 calibration only) 8x60ml for Cl determination 8x _ 40ml samples for nutrient determination 8x1l filtered adicified samples

---

STATION REPORT

Station No.:	**357 SL**
Sampler type:	sediment corer
Area:	Palinuro Smt
Date:	04.05.93
Latitude:	39°32'43N
Longitude:	14°42'42E
Water depth:	615m
Station time (UTC):	16:39-17:00
Total time (min):	21
Remarks:	
Samples:	110cm sediment core of layer; top cm soft, brown; upper layer grey, solid

STATION REPORT

Station No.:	**358 SL**
Sampler type:	sediment corer
Area:	Palinuro Smt
Date:	04.05.93
Latitude:	39°32'45N
Longitude:	14°42'37E
Water depth:	622m
Station time (UTC):	17:15-17:34
Total time (min):	19
Remarks:	
Samples:	sediment of 160cm layer, as above, H_2S-smell

STATION REPORT

Station No.:	**359 MS**
Sampler type:	multiprobe + water rosette
Area:	Lipari
Date:	05.05.93
Latitude:	38°25'03N
Longitude:	15°02'27E
Water depth:	734m
Station time (UTC):	14:47
Total time (min):	15
Remarks:	
Samples:	no samples

STATION REPORT

Station No.:	**360 MS**
Sampler type:	multiprobe + water rosette
Area:	Lipari
Date:	05.05.93
Latitude:	38°25'10N
Longitude:	15°02'82E
Water depth:	925m
Station time (UTC):	15:32
Total time (min):	15
Remarks:	
Samples:	no samples

STATION REPORT

Station No.:	**361 DS**
Sampler type:	dredge
Area:	Lipari
Date:	05.05.93
Latitude:	38°24'88N
Longitude:	15°02'23E
Water depth:	755m
Station time (UTC):	16:06-17:11
Total time (min):	65
Remarks:	
Samples:	carbonate crust, covered with Mn

STATION REPORT

Station No.:	**362 MS**
Sampler type:	multiprobe + water rosette
Area:	Marsilli Smt
Date:	06.05.93
Latitude:	39°17'02N
Longitude:	14°23'65E
Water depth:	569m
Station time (UTC):	6:00-6:19
Total time (min):	19
Remarks:	
Samples:	HC5-1 - HC5-8 8x5l water samples 8x60ml for Cl determination 8x _ 40ml samples for nutrient determination 8x1l filtered acidified samples

---

STATION REPORT

Station No.:	**363**
Sampler type:	dredge
Area:	Marsilli Smt
Date:	06.05.93
Latitude:	39°17'00N
Longitude:	14°23'45E
Water depth:	784m
Station time (UTC):	6:52-7:48
Total time (min):	56
Remarks:	loss of dredge
Samples:	

STATION REPORT

Station No.:	**364 BG**
Sampler type:	sediment grab
Area:	Marsilli Smt
Date:	06.05.93
Latitude:	39°17'04
Longitude:	14°23'90
Water depth:	530m
Station time (UTC):	9:13-9:29
Total time (min):	16
Remarks:	
Samples:	no sediments

STATION REPORT

Station No.:	**365 BG**
Sampler type:	sediment grab
Area:	Marsilli Smt
Date:	06.05.93
Latitude:	39°17'04N
Longitude:	14°23'71E
Water depth:	530m
Station time (UTC):	9:42-9:51
Total time (min):	9
Remarks:	
Samples:	coarse grained sand with red fragments (Fe-hydroxid fragments); volcanic material

STATION REPORT

Station No.:	**366 OFOS**
Sampler type:	extended OFOS
Area:	Marsilli Smt
Date:	06.05.93
Latitude:	39°17'35N
Longitude:	14°23'54E
Water depth:	660m
Station time (UTC):	10:45-17:19
Total time (min):	394
Remarks:	
Samples:	1 piece of lava on top of the OFOS frame, covered with corals and Mn coated; 604 photos, 394 min of video

---

STATION REPORT

Station No.:	**367 OFOS**
Sampler type:	extended OFOS
Area:	Palinuro Smt
Date:	07.05.93
Latitude:	39°31'74N
Longitude:	14°38'20E
Water depth:	690m
Station time (UTC):	7:13-10:12
Total time (min):	179
Remarks:	
Samples:	300 photos, 179 min of video

STATION REPORT

Station No.:	**368**
Sampler type:	Transponder
Area:	Palinuro Smt
Date:	
Latitude:	see transponder report
Longitude:	
Water depth:	
Station time (UTC):	
Total time (min):	
Remarks:	recovery of 5 transponder
Samples:	

STATION REPORT

Station No.:	**369 SL**
Sampler type:	gravity corer
Area:	Palinuro Smt
Date:	07.05.93
Latitude:	39°31'36N
Longitude:	14°39'76E
Water depth:	662m
Station time (UTC):	14:25-14:48
Total time (min):	23
Remarks:	
Samples:	80cm, green-gray endurated clay, pieces (2-3mm) of Fe-hydroxide and very small Mn-nodules, some muscorite; top cm = light brown soft mud.

STATION REPORT

Station No.:	**370 WS**
Sampler type:	niskin water sampler
Area:	Eolian Islands
Date:	08.05.93
Latitude:	38°38'30N
Longitude:	15°06'30E
Water depth:	27m
Station time (UTC):	11:00-13:00
Total time (min):	120
Remarks:	Hydrothermal spot between Datiilo and Lisca Bianca to the west of Panakea island. Also the samples.
Samples:	P1 - P4 4x5l water samples 4x _ 30ml for Cl determination 4x _ 40ml samples for nutrient determination 4x1l filtered acidified samples 4x60ml for H_2S determination

---

STATION REPORT

Station No.:	**371 OFOS**
Sampler type:	extended OFOS
Area:	Baziluzzo
Date:	08.05.93
Latitude:	38°39'92N
Longitude:	15°06'11E
Water depth:	67m
Station time (UTC):	15:47-17:25
Total time (min):	98
Remarks:	
Samples:	334 Photos

STATION REPORT

Station No.:	**372 WS**
Sampler type:	niskin water samples
Area:	Panarea
Date:	08.05.93
Latitude:	38°39'97N
Longitude:	15°06'04E
Water depth:	ca. 67m
Station time (UTC):	17:30
Total time (min):	
Remarks:	near bottom water, where echo-sounder anomalies had been observed.
Samples:	HC6-1; HC6-4 2x5l water samples 2x1l filtered acidified samples

---

STATION REPORT

Station No.:	**373 Profil**
Sampler type:	echosounder
Area:	Eolian Islands
Date:	08.05.93
Latitude:	
Longitude:	
Water depth:	
Station time (UTC):	
Total time (min):	
Remarks:	
Samples:	

STATION REPORT

Station No.:	**374 profil**
Sampler type:	echosounder
Area:	Eolian Islands
Date:	08.05.93
Latitude:	
Longitude:	
Water depth:	
Station time (UTC):	
Total time (min):	
Remarks:	
Samples:	

STATION REPORT

Station No.:	**375 OFOS**
Sampler type:	extended OFOS
Area:	Salina
Date:	09.05.93
Latitude:	38°28'8N
Longitude:	14°30'9E
Water depth:	100m
Station time (UTC):	11:55
Total time (min):	
Remarks:	
Samples:	photos, videos

STATION REPORT

Station No.:	**376 WS**
Sampler type:	niskin water sampler
Area:	Baziluzzo
Date:	09.05.93
Latitude:	38°30'63N
Longitude:	14°53'64E
Water depth:	115m
Station time (UTC):	13:50-15:30
Total time (min):	100
Remarks:	
Samples:	B2 1x5l water samples 1x60ml for Cl determination 1x _ 40ml samples for nutrient determination 1x1l filtered acidified samples

---

STATION REPORT

Station No.:	**377 WS**
Sampler type:	niskin water sampler
Area:	Baziluzzo
Date:	09.05.93
Latitude:	38°31'3N
Longitude:	14°54'3E
Water depth:	92m
Station time (UTC):	15:39
Total time (min):	
Remarks:	
Samples:	B4 1x5l water samples 1x60ml for Cl determination 1x _ 40ml samples for nutrient determination 1x1l filtered acidified samples

STATION REPORT

Station No.:	**378 BG**
Sampler type:	sediment grab
Area:	Baziluzzo
Date:	09.05.93
Latitude:	38°29'9N
Longitude:	14°53'3E
Water depth:	105
Station time (UTC):	16:02
Total time (min):	
Remarks:	
Samples:	black sandy sediment

STATION REPORT

Station No.:	**379 BG**
Sampler type:	sediment grab
Area:	Baziluzzo
Date:	09.05.93
Latitude:	38°29'05N
Longitude:	14°52'97E
Water depth:	106
Station time (UTC):	16:23
Total time (min):	
Remarks:	
Samples:	black sandy sediments with Fe-crusts

STATION REPORT

Station No.:	**380 profil**
Sampler type:	echosounding profiles
Area:	Vulcano
Date:	10.05.93
Latitude:	38°22'48N
Longitude:	14°58'98E
Water depth:	100m
Station time (UTC):	8:18-9:21
Total time (min):	63

Remarks:

Samples:

STATION REPORT

Station No.:	**381**
Sampler type:	rubber boat
Area:	Vulcano
Date:	10.05.93
Latitude:	38°22N
Longitude:	14°54E
Water depth:	_ 100m
Station time (UTC):	
Total time (min):	

Remarks:

Samples:

STATION REPORT

Station No.:	**382 OFOS**
Sampler type:	extended OFOS
Area:	Vulcano
Date:	10.05.93
Latitude:	38°25'38N
Longitude:	14°56'11E
Water depth:	144m
Station time (UTC):	10:56-11:38
Total time (min):	42
Remarks:	
Samples:	photos, videos

STATION REPORT

Station No.:	**383**
Sampler type:	rubber boat
Area:	Vulcano
Date:	10.05.93
Latitude:	
Longitude:	
Water depth:	
Station time (UTC):	
Total time (min):	
Remarks:	
Samples:	

STATION REPORT

Station No.:	**384 OFOS**
Sampler type:	extended OFOS
Area:	Vulcano
Date:	10.05.93
Latitude:	38°26'N
Longitude:	14°58'E
Water depth:	
Station time (UTC):	
Total time (min):	
Remarks:	tests
Samples:	

Appendix 2: Multiprobe profiles

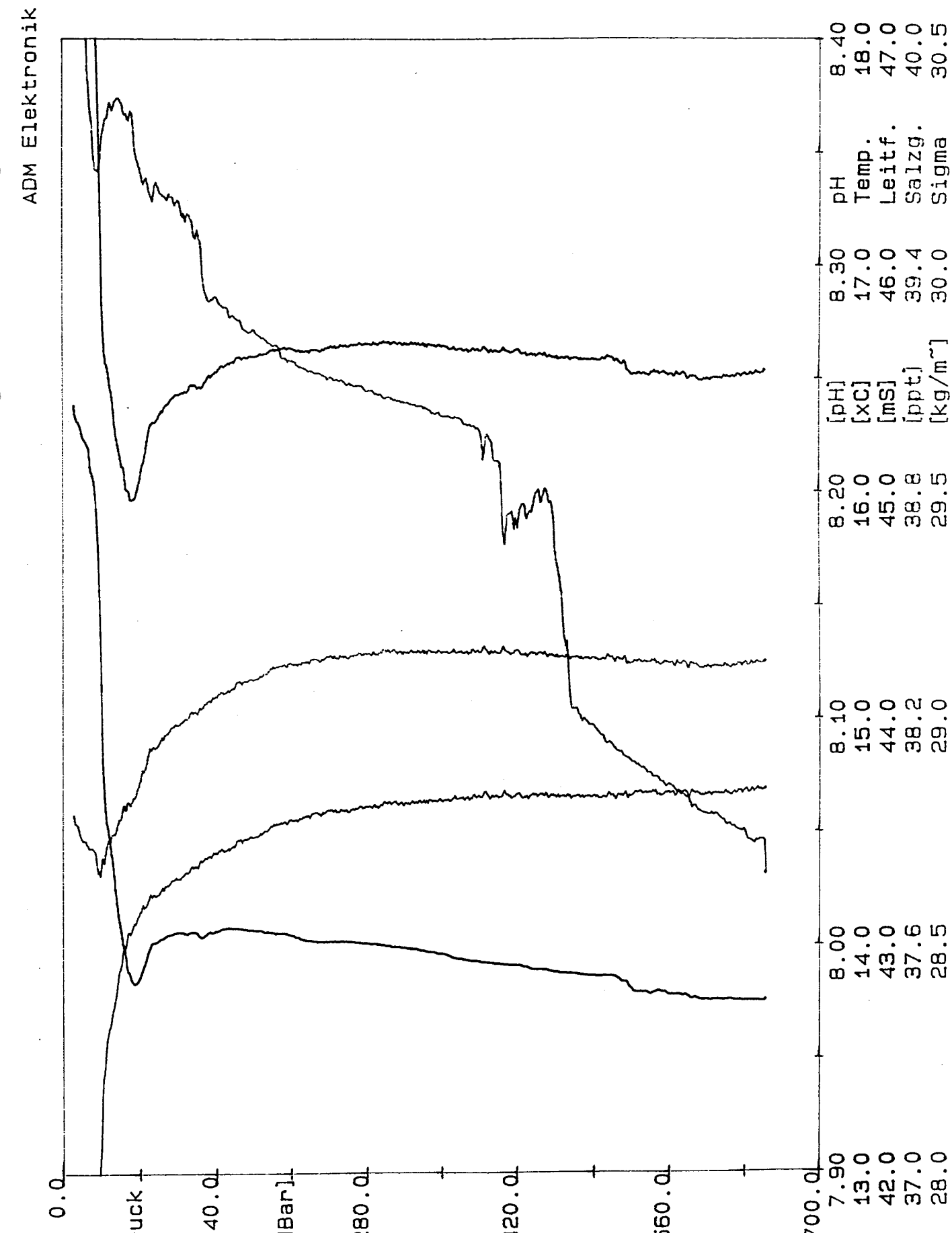

Pos 200-4 - Stat 346 - HC2 - W. Palinuro

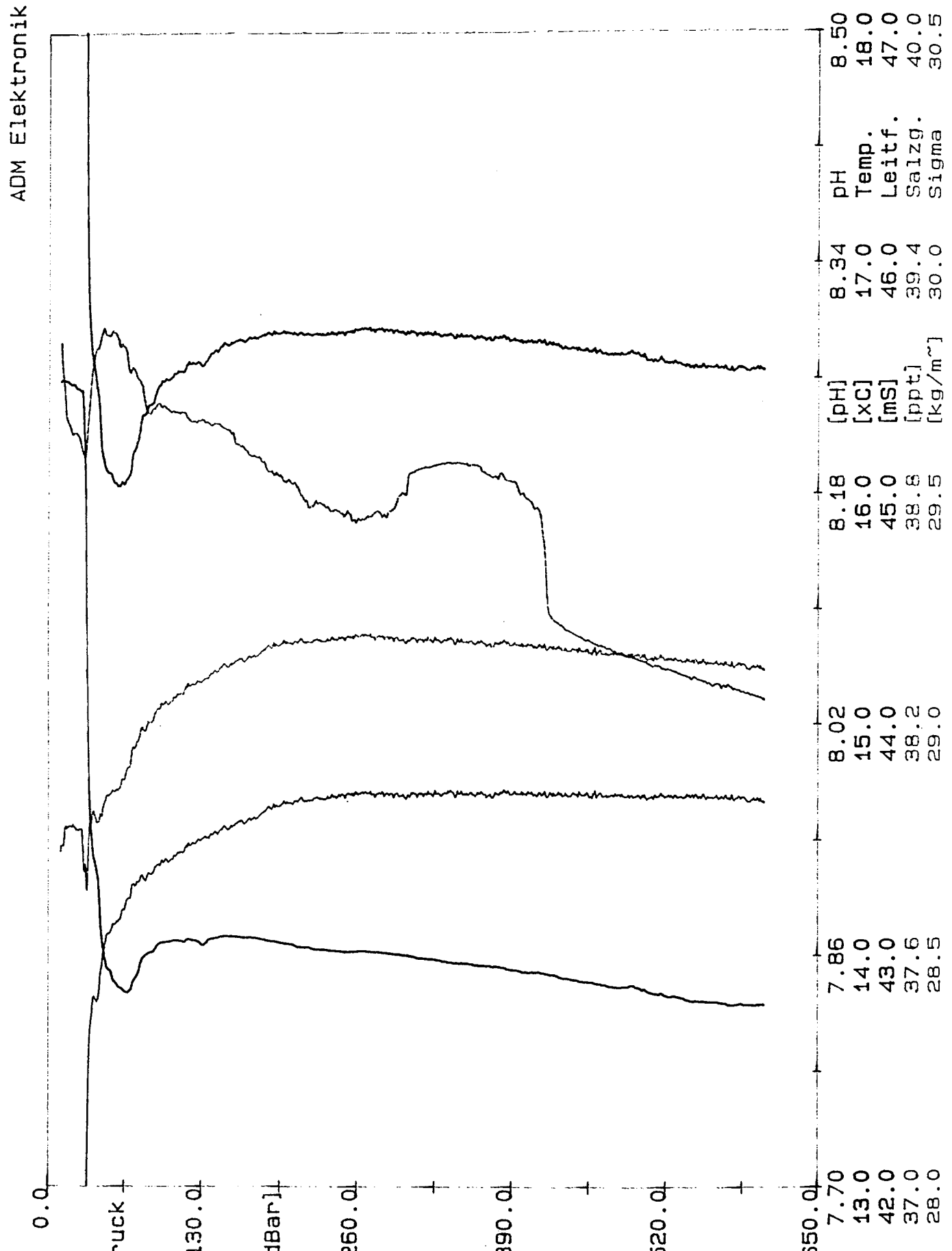

Pos 200-4 - Stat 353 - HC3 - W. Palinuro

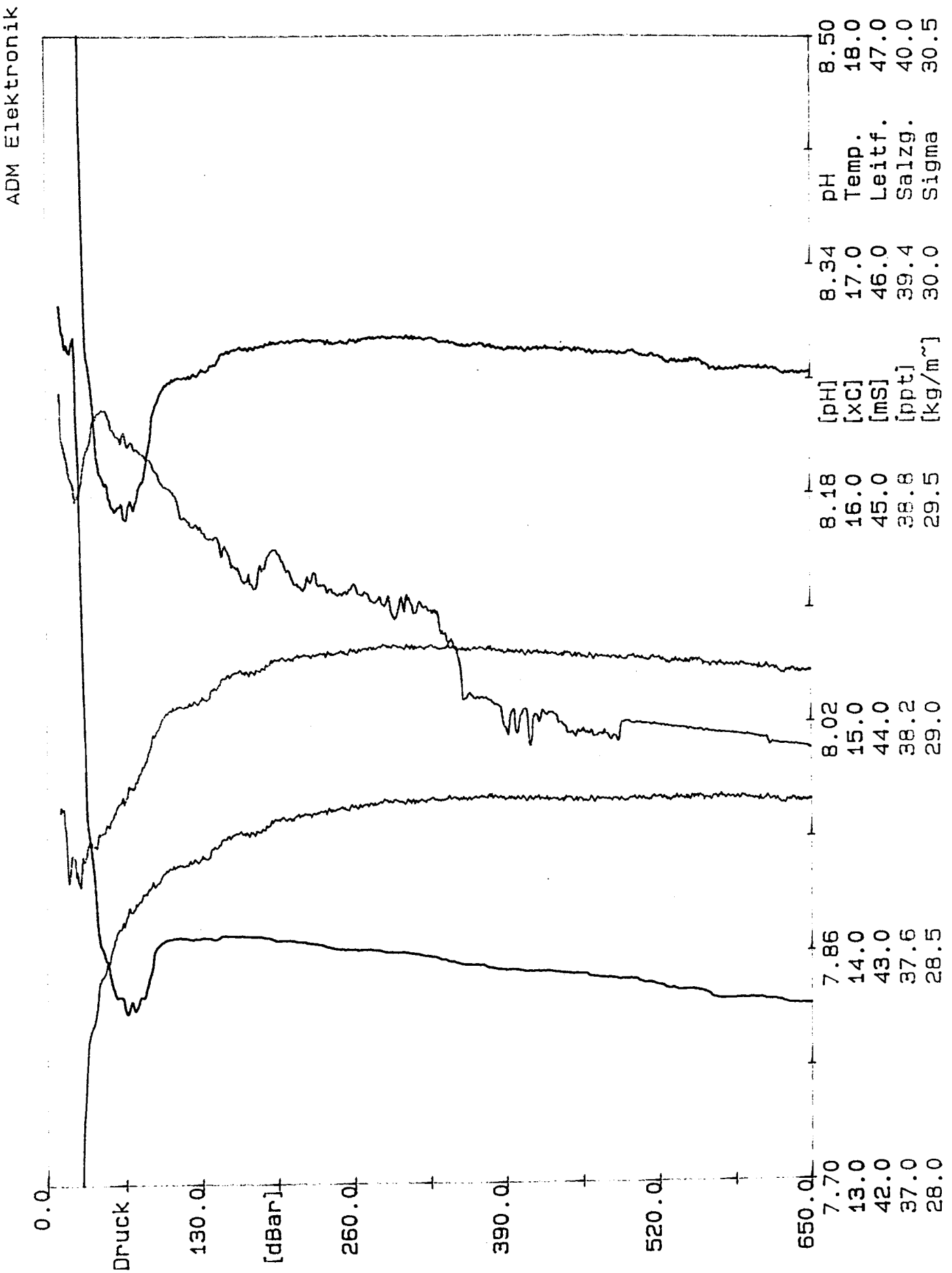

Pos 200-4 - Stat 353 - HC3 - W. Palinuro

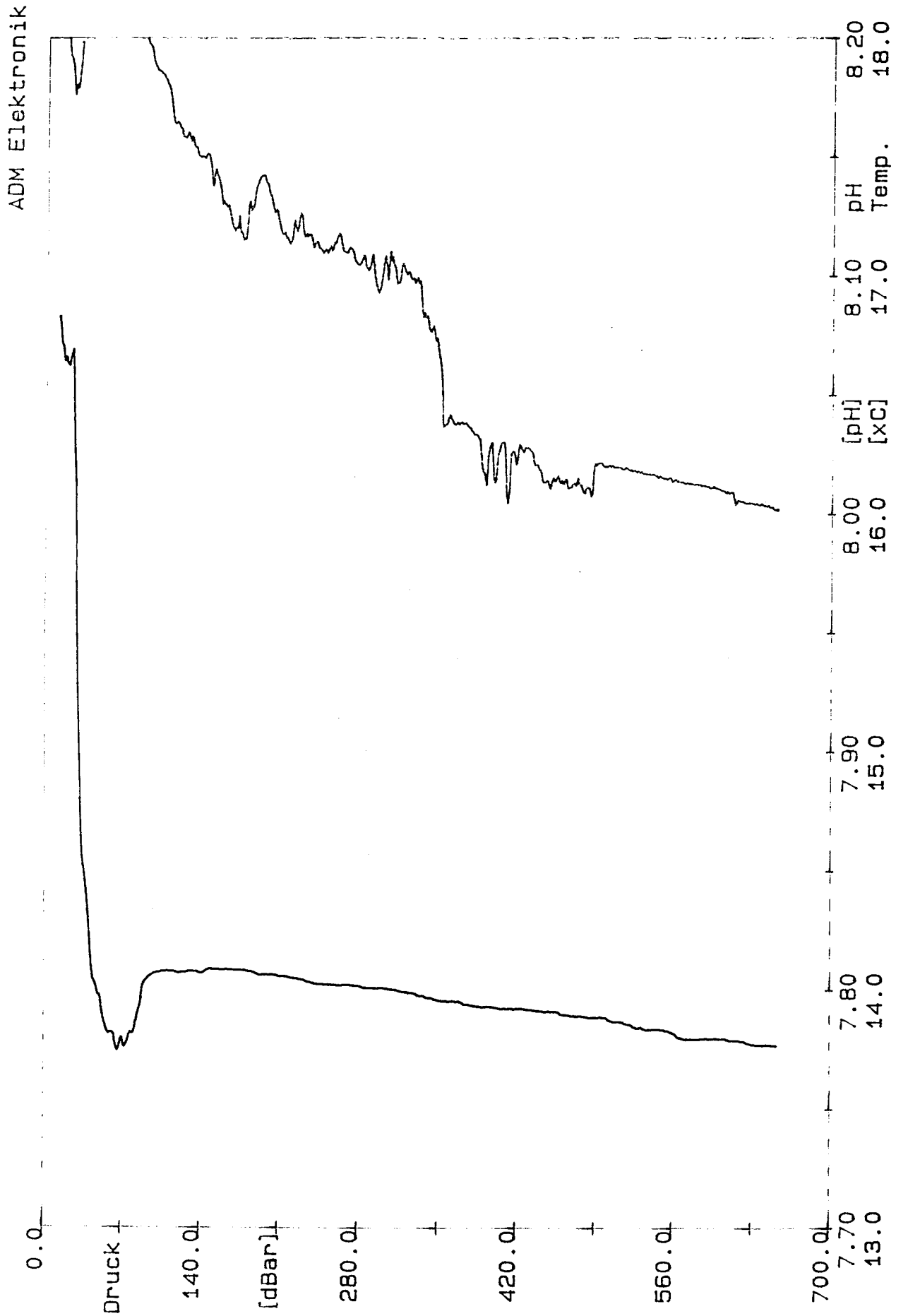

Pos 200-4 - Stat 356 - HC4 - E. Palinuro

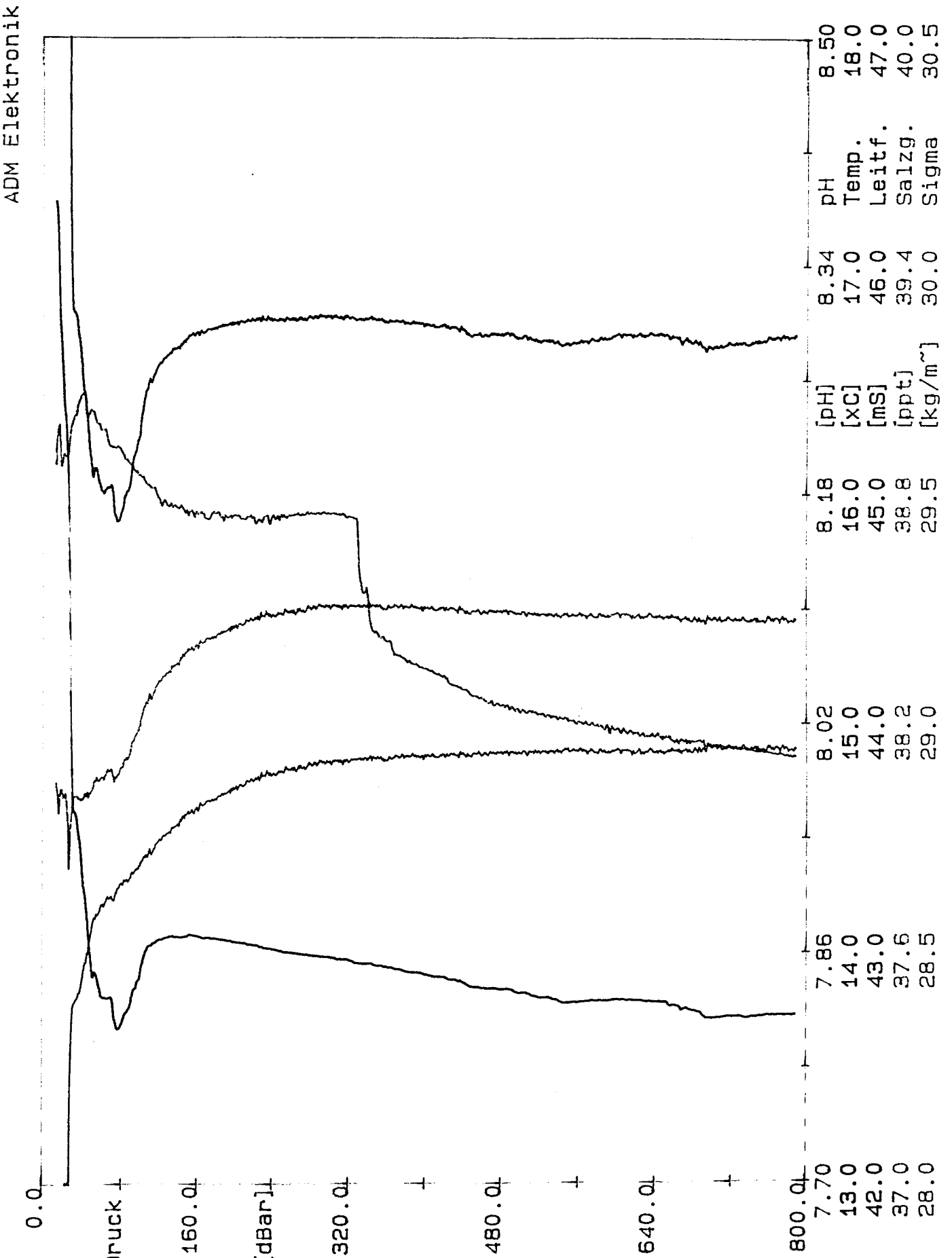

Pos 200-4 - Stat 362 - HC5 - Marsilli

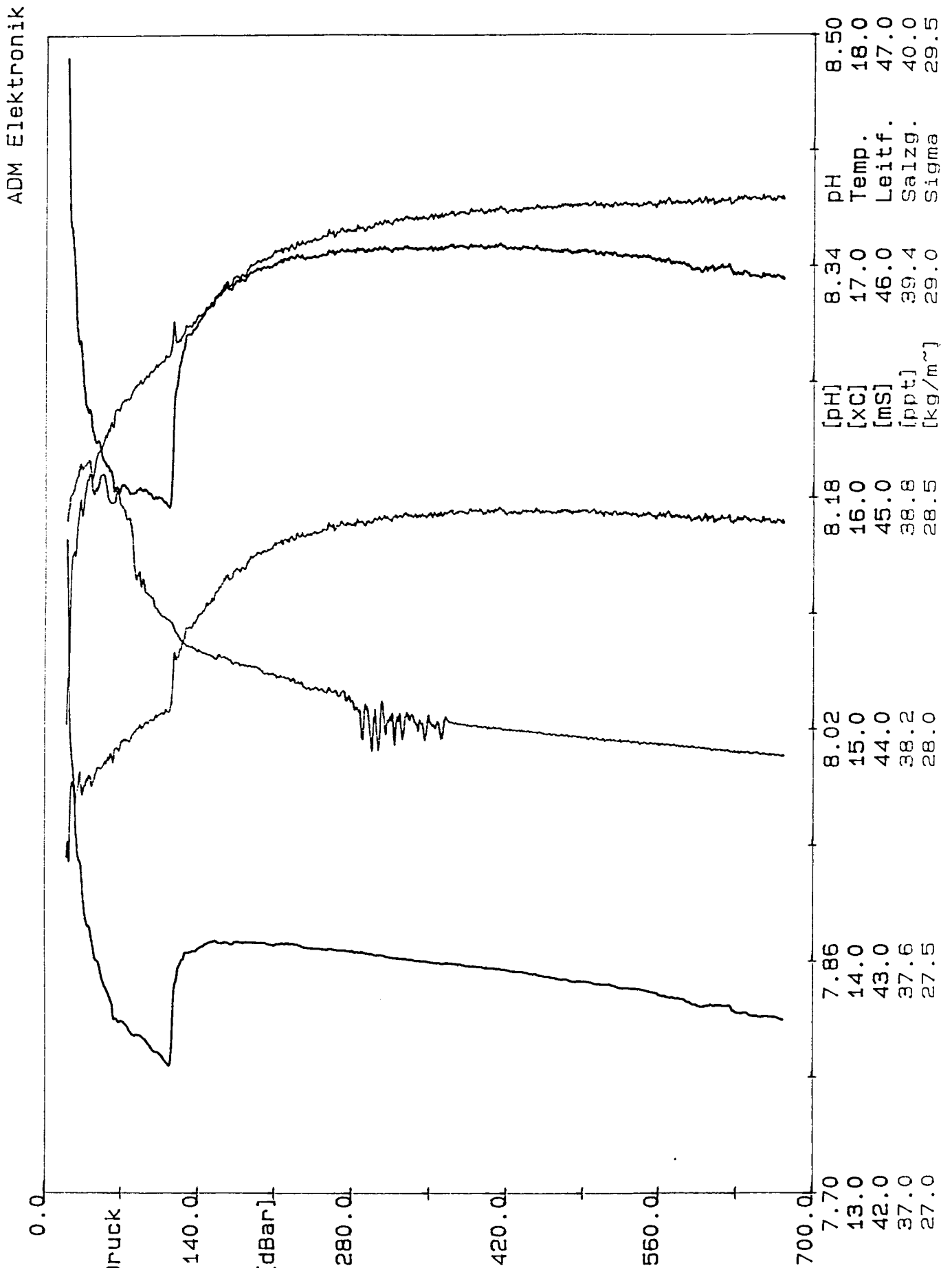

Appendix 3: Chemical results of Vulcano fluids

Major and minor element concentrations in bend waters of Vulcano

Sample	Date	Sample Site/ Comments	T (C°)	Cl mmol/l	Si µmol/kg	Ca mmol/kg	Mg mmol/kg	Sr µmol/kg	Fe µmol/kg	Mn µmol/kg
V 1	05.05.93	beach ambient	21.5	586.3	88.2	11.20	56.49	66	1.19	1.28
V 2	"	beach ambient	21.5	585.5	87.5	11.18	56.54	66	1.30	1.32
V 3	"	beach fumarole 1	65.5	550.6	1633.3	10.47	51.95	52	8.92	19.86
V 4	"	beach fumarole 1	63.0	549.4	1423.7	10.53	52.13	50	5.33	19.95
V 5	"	beach fumarole 1	54.0	561.0	1237.7	10.83	53.40	55	5.77	16.52
V 6	"	beach fumarole 1	44.0	570.6	770.6	11.17	54.58	57	7.92	11.99
V 7	10.05.93	hot sands	25.5	582.7	529.1	12.36	59.15	63	58.05	84.75
V 8	"	hot sands	24.5	583.8	483.5	12.97	58.16	62	48.24	79.62
V 9	"	hot sands ambient	19.0	585.5	75.5	11.19	56.88	65	0.52	9.68
V 10	"	beach fumarole 2	40.0	566.9	630.8	11.05	53.93	61	4.97	6.38
V 11	"	beach fumarole 2	54.5	549.7	800.7	10.93	52.93	60	2.66	11.22
V 17	"	beach fumarole 2	51.5	552.2	731.8	10.89	52.20	59	4.67	9.95
V 18	"	beach ambient	19.0	587.7	46.6	11.12	56.80	66	55.99	0.78

= Beim Öffnen der Flaschen starker H_2S-Geruch, sowie Schwefelausfällungen in der Flasche.

Nutrient concentrations in water samples of the Pos 200-4 cruise

Sample	Date	Sample Site/ Comments	T (C°)	NO_2 µM/l	NH_4 µM/l	NO_3 µM/l	PO_4 µM/l	SO_4 mM/l	O_2 nmol/kg	H_2S µmol/kg	pH NBS	A meq/k uncor
V..1	05.05.93	beach ambitent	21.5	0.01	17.60	0.17	0.04	-	-	-	6.5	2.5
V 2	"	beach ambient	21.5	0.00	21.60	0.08	0.04	-	-	-	6.5	2.5
V 3	"	beach										
		fumarole 1	65.5	0.00	640.00	0.05	1.10*	29.54	-	-	5.6	1.9
V 4	"	beach										
		fumarole 1	63.0	0.00	658.00	0.00	1.23*	29.21	-	-	5.9	1.9
V 5	"	beach										
		fumarole 1	54.0	0.00	438.00	0.02	0.58*	43.54	-	-	5.7	2.1
V 6	"	beach										
		fumarole 1	44.0	0.01	253.00	0.08	0.13*	-	-	-	6.1	2.3
V 7	10.05.93	hot sands	25.5	0.00	30.00	0.09	0.05	34.32	-	-	6.2	2.0
V 8	"	hot sands	24.5	0.01	28.40	0.04	0.04	-	-	-	6.3	2.0
V 9	"	hot sands										
		ambient	19.0	0.01	3.60	0.03	0.10	32.01	-	-	7.5	2.4
V 10	"	beach										
		fumarole 2	40.0	0.01	330.00	0.03	0.75*	-	-	-	5.5	2.0
V 11	"	beach										
		fumarole 2	54.5	0.00	428.00	0.02	1.32*	30.15	-	-	5.7	1.9
V 17	"	beach										
		fumarole 2	51.5	0.01	380.00	0.01	1.26*	-	-	-	5.5	1.9
V 18	"	beach ambient	19.0	0.01	13.00	0.03	0.56	-	-	-	7.1	2.5

* = Beim Öffnen der Flaschen starker H_2S-Geruch, sowie Schwefelausfällungen in der Flasche.

Nutrient concentrations in water samples of the Pos 200-4 cruise

Sample	Date	Sample Site/ Comments	T (C°)	NO_2 µM/l	NH_4 µM/l	NO_3 µM/l	PO_4 µM/l	SO_4 µM/l	O_2 nmol/kg	H_2S µmol/kg	pH NBS	AT meq/kg uncorr
VF1	05.05.93	beach ambient field pH		-	-	-	-	-	-	-	6.1	-
VF2	"	beach fumarole 1 field pH		-	-	-	-	-	-	-	5.2	-
V1S	"	beach ambient for H_2S		-	-	-	-	-	-	-	153.3	-
V2S	"	beach fumarole 1 for H_2S		-	-	-	-	-	-	-	272.5	-
VO1	"	beach ambient for O_2		-	-	-	-	-	-	0.28	-	-
VO2	"	beach fumarole 1 for O_2		-	-	-	-	-	-	0.04	-	-
VF3	10.05.93	beach fumarole 2 field pH		-	-	-	-	-	-	-	5.4	-
V16	"	beach fumarole 2 for H_2S		-	-	-	-	-	-	-	166.0	-
VO3	"	beach fumarole 2 for O_2		-	-	-	-	-	-	0.11	-	-